The *Arabidopsis* SR45 Splicing Factor, a Negative Regulator of Sugar Signaling, Modulates SNF1-Related Protein Kinase 1 (SnRK1) Stability

Raquel F. Carvalho,[a,1] Dóra Szakonyi,[a] Craig G. Simpson,[b] Inês C.R. Barbosa,[a,2] John W.S. Brown,[b,c] Elena Baena-González,[a] and Paula Duque[a,3]

[a] Instituto Gulbenkian de Ciência, Rua da Quinta Grande, 6, 2780-156 Oeiras, Portugal

[b] The James Hutton Institute, Invergowrie, Dundee DD2 5DA, Scotland, UK

[c] University of Dundee at The James Hutton Institute, Invergowrie, Dundee DD2 5DA, Scotland, UK

Running head: SR45 Modulates SnRK1 Stability

[1] Current address: Horticultural Sciences Department, University of Florida, Gainesville, FL 32611, USA

[2] Current address: Department of Plant Systems Biology, Center for Life and Food Sciences Weihenstephan, Technische Universität München, 85354 Freising, Germany

[3] Address correspondence to duquep@igc.gulbenkian.pt

The author responsible for distribution of materials integral to the findings presented in this article in accordance with the policy described in the Instructions for Authors (www.plantcell.org) is: Paula Duque (duquep@igc.gulbenkian.pt).

ABSTRACT

The ability to sense and respond to sugar signals allows plants to cope with environmental and metabolic changes by adjusting growth and development accordingly. We previously reported that the SR45 splicing factor negatively regulates glucose signaling during early seedling development in *Arabidopsis thaliana*. Here, we show that under glucose-fed conditions the *Arabidopsis sr45-1* loss-of-function mutant contains higher amounts of the energy-sensing SNF1-Related Protein Kinase 1 (SnRK1) despite unaffected *SnRK1* transcript levels. In agreement, marker genes for SnRK1 activity are upregulated in *sr45-1* plants, and the glucose hypersensitivity of *sr45-1* is attenuated by disruption of the *SnRK1* gene. Using a high-resolution RT-PCR panel, we found that the *sr45-1* mutation broadly targets alternative splicing in vivo, including that of the *SR45* pre-mRNA itself. Importantly, the enhanced SnRK1 levels in *sr45-1* are suppressed by a proteasome inhibitor, indicating that SR45 promotes targeting of the SnRK1 protein to proteasomal destruction. Finally, we demonstrate that SR45 controls alternative splicing of the *Arabidopsis 5PTase13* gene, which encodes an inositol polyphosphate 5-phosphatase previously shown to interact with and regulate the stability of SnRK1 in vitro, thus providing a mechanistic link between SR45 function and the modulation of degradation of the SnRK1 energy sensor in response to sugars.

INTRODUCTION

Higher plants are able to transduce sugar signals in order to adjust developmental programs, maintain energy homeostasis and achieve stress tolerance in response to metabolic and environmental fluctuations. Glucose, in addition to being a carbon and energy source, plays an important regulatory role as a central signaling molecule, modulating gene expression and influencing a variety of processes such as germination, early seedling development, flowering or senescence (Koch, 1996; Gibson, 2005; Rolland et al., 2006). The glycolytic enzyme hexokinase (HXK) is an evolutionarily conserved glucose sensor, operating as a dual-function enzyme with both catalytic and regulatory roles. Indeed, the characterization of loss-of-function, overexpression and catalytically inactive *HXK1* lines (Jang et al., 1997; Dai et al., 1999; Moore et al., 2003) has established HXK1 as a true glucose sensor in plants while demonstrating that glucose signaling can be uncoupled from glucose metabolism. Genetic studies in *Arabidopsis thaliana* have also suggested the existence of a HXK1-independent pathway for glucose signal transduction (Xiao et al., 2000). On the other hand, the highly conserved Sucrose Non-Fermenting 1 (SNF1)-related protein kinases 1 (SnRK1s) sense stress-associated energy deprivation and reprogram transcription to restore homeostasis and promote plant stress tolerance (Radchuk et al., 2006; Baena-Gonzalez et al., 2007; Lee et al., 2009). Extensive links between SnRK1 signaling and the abscisic acid (ABA) stress pathway have been uncovered, with *SnRK1* overexpression altering plant sensitivity to both glucose and ABA (Jossier et al., 2009; Tsai and Gazzarrini, 2012). The demonstration that SnRK1 is inactivated by type 2C protein phosphatases, established repressors of the ABA pathway, has provided a molecular explanation for the long-recognized crosstalk between sugar and ABA signaling (Rodrigues et al., 2013).

SR45 is an RNA-binding protein highly conserved in the plant kingdom that has been shown to function as an essential splicing factor due to its ability to complement a mammalian extract deficient in serine/arginine-rich (SR) proteins (Ali et al., 2007) and had hence been regarded as a member of this important family of alternative splicing regulators (Lin and Fu, 2007). However, owing to its highly atypical SR protein structure — a single RNA recognition motif (RRM) flanked by two arginine/serine-rich (RS) domains, instead of one or two N-terminal RRMs and a downstream RS domain — SR45 is no

longer included in the *Arabidopsis* SR protein family (Barta et al., 2010). It is a close homolog of the human RNA-binding protein S1 (RNPS1) (Pendle et al., 2005; Zhang and Mount, 2009), a versatile splicing activator and component of the exon-exon junction complex (Mayeda et al., 1999; Le Hir et al., 2001; Sakashita et al., 2004) implicated in mRNA nuclear export, nonsense mediated decay and genome stability (Lykke-Andersen et al., 2001; Li et al., 2007). The domain organization of the *Arabidopsis* SR45 protein is also strikingly similar to that of the human SR-like Tra2β splicing factor, which has been associated with several types of cancer and neuronal disorders (Kiryu-Seo et al., 1998; Jiang et al., 2003; Watermann et al., 2006; Gabriel et al., 2009; Kajita et al., 2013).

The *A. thaliana* SR45 was first identified in a yeast two-hybrid screen as an interacting partner of U1-70K (Golovkin and Reddy, 1999), a component of the U1 small nuclear ribonucleoprotein (snRNP) known in animals to initiate spliceosome assembly by binding the 5' pre-mRNA splice site (Zhuang and Weiner, 1986; Kohtz et al., 1994). Interestingly, Day et al. (2012) have also reported an interaction between SR45 and the spliceosomal factor U2AF^{35}, which in metazoans is involved in 3' splice site recognition (Wu et al., 1999; Wahl et al., 2009). Moreover, SR45 has been found to interact with three U5 snRNP proteins (Zhang et al., 2014) as well as with several other *Arabidopsis* SR proteins, namely SCL33, RSZ21, SR30, SR34 and SR34a (Golovkin and Reddy, 1999; Zhang et al., 2014; Stankovic et al., 2016). Another two reported SR45-interacting proteins in *Arabidopsis* are the spliceosomal component SKIP (Wang et al., 2012), which confers salt stress tolerance (Feng et al., 2015), and CACTIN, an essential nuclear factor required for embryogenesis (Baldwin et al., 2013). Early studies had shown that AFC2, a LAMMER-type protein kinase, is able to interact with and phosphorylate SR45 in vitro (Golovkin and Reddy, 1999) and found SR45 to be confined to the nucleus, either diffusely distributed in the nucleoplasm or concentrated in speckles, with its subnuclear dynamics being regulated by phosphorylation, ATP and transcription (Ali et al., 2003; Ali and Reddy, 2006). However, recently reported evidence substantiates nucleo-cytoplasmic shuttling activity for SR45, with possible involvement of the nuclear exporter protein XPO1 (Stankovic et al., 2016).

As many other splicing-related components, the *Arabidopsis SR45* gene itself undergoes alternative splicing, generating two splice variants, *SR45.1* and *SR45.2*, that differ by an in-frame 21-nt sequence as a result of an alternative 3' splice site selection

event (Palusa et al., 2007; Zhang and Mount, 2009). A third *SR45* splice variant arising from selection of an alternative 5' splice site and including 33 nt absent from the other two transcripts has been recently annotated but its expression pattern and significance remain unknown. First insights into the in vivo roles of *SR45* stemmed from the characterization of the *Arabidopsis* T-DNA insertion mutant, *sr45-1*. Reddy and co-workers initially reported that this loss-of-function allele displays pleiotropic developmental defects, including reduced plant size, delayed flowering, altered leaf and flower morphology, as well as slower root growth (Ali et al., 2007). Remarkably, expression of the longest of the two characterized *SR45* splice variants (*SR45.1*) in the mutant background only rescues the floral morphology phenotype while the shortest (*SR45.2*) complements exclusively the delay in root growth, demonstrating that the two splice forms fulfill distinct physiological roles (Zhang and Mount, 2009). The first endogenous SR45 splicing targets identified encoded *Arabidopsis* SR proteins (Ali et al., 2007) and indeed SR45 was later shown to interact with an intronic region of the *SR30* gene (Day et al., 2012), providing the first evidence for direct binding of this SR-like splicing factor to a native pre-mRNA sequence. Zhang et al. (2014) subsequently reported that phosphorylation of a specific amino acid (T218) present only in the SR45.1 isoform is key to both its distinctive function in flower petal development and splicing regulation of the direct SR45 target, *SR30*. More recently, SR45 was shown to also bind directly to an intronic region of *CCA1*, encoding a master circadian clock regulator (Filichkin et al., 2015). Interestingly, one study has implicated SR45 in siRNA-mediated DNA methylation and gene silencing in *Arabidopsis* (Ausin et al., 2012).

A genome-wide analysis using RNA immunoprecipitation followed by highthroughput sequencing (RIP-seq) has very recently identified more than 4,000 RNAs associated with SR45 in *Arabidopsis* seedlings, many of which unexpectedly derive from intronless genes (Xing et al., 2015). These SR45-bound RNAs were evidently enriched in genes functioning in hormone and stress signaling pathways, most particularly in components of the ABA network. This is in agreement with our previous report that, in addition to its functions in normal plant development, the *Arabidopsis* SR45 protein negatively regulates glucose signaling by repressing the ABA pathway (Carvalho et al., 2010). In fact, the *sr45-1* mutation causes hypersensitivity to glucose during early seedling growth by enhancing the

ability to accumulate ABA in response to the sugar, with ABA biosynthesis and signaling genes being overinduced by glucose in *sr45-1* plants. We also showed that both the *SR45.1* and *SR45.2* transcripts are capable of rescuing the mutant's sugar phenotype, indicating that alternative splicing does not play a role in this response (Carvalho et al., 2010). However, the exact molecular mechanisms governing the mode of action of SR45 in sugar signaling remained to be elucidated.

Here, we show that, while not affecting total transcript levels or alternative splicing of the *SnRK1.1* gene, SR45 is involved in glucose-responsive modulation of SnRK1.1 protein degradation. In line with this, SR45 controls alternative splicing of the *5PTase13* gene, which encodes an inositol polyphosphate 5-phosphatase previously shown to interact with and regulate the stability of the SnRK1.1 protein in vitro (Ananieva et al., 2008). We have also identified several additional splicing targets of the SR-related SR45 protein in *Arabidopsis*, which likely include *SR45* itself.

RESULTS

Glucose Hypersensitivity Caused by Loss of *SR45* Function Is Unaffected by Disruption of HXK1 Signaling

Our previous finding that the *Arabidopsis sr45-1* mutant is hypersensitive to glucose during early seedling development (Carvalho et al., 2010) prompted us to investigate the dependency of this phenotype on signal transduction mediated by the evolutionarily conserved HXK1 glucose sensor.

We first examined whether the *sr45-1* mutation affects expression of the *HXK1* gene, which in agreement to the current genome annotation (TAIR10; www.arabidopsis.org) was found to generate a single transcript. As shown in the real-time RT-qPCR analysis of Figure 1A, and consistent with a previous global microarray-based transcriptome analysis (Price et al., 2004), exogenous glucose induced *HXK1* expression. However, glucose regulation of the *HXK1* gene was unaffected in the *sr45-1* mutant background (Figure 1A).

We next used a genetic approach and generated double mutants in which both the *SR45* and *HXK1* genes are disrupted. The *sr45-1* mutant is in the Col-0 background, whereas the most extensively characterized null mutant for *HXK1*, *gin2-1*, was isolated via

EMS mutagenesis of L*er* ecotype seeds (Moore et al., 2003). To obviate problems in the double mutant phenotypic analysis arising from different parental ecotypes, instead of the original *gin2-1* mutant we made use of two Col-0 background mutant lines for *HXK1, hxk1-1* and *hxk1-2* (Aki et al., 2007). Both mutant alleles harbor T-DNA insertions in the first intron of the *HXK1* gene. However, RT-PCR analysis using a primer pair flanking the insertions revealed that the *HXK1* transcript is below detectable levels in *hxk1-1*, suggesting that this is a null mutant, while *hxk1-2* exhibits a reduction in *HXK1* mRNA levels (see Supplemental Figure 1A). Nevertheless, consistent with an earlier report (Aki et al., 2007), our results indicate that both these single mutant lines display glucose insensitivity during early seedling development (Figures 1B to 1E), as expected from the loss of function or knock down of a critical component in the sensing of glucose levels.

Notably, disruption of the *HXK1* gene did not affect the glucose oversensitive phenotypes conferred by the *sr45-1* mutation. In the presence of sugar, *sr45-1* seedlings exhibit an early growth arrest, with cotyledon development being strikingly impaired in comparison to the wild type (Carvalho et al., 2010) (Figures 1B and 1C). Figures 1B and 1C show that, in the presence of 4% glucose, the *sr45-1 hxk1-1* and the *sr45-1 hxk1-2* double mutants displayed a similar reduction in cotyledon greening. Additionally, the *sr45-1* mutant, which is affected in general development and hence shows shorter hypocotyls under control conditions, displays increased sensitivity to the glucose inhibitory effects on hypocotyl elongation of dark-grown seedlings (Carvalho et al., 2010) (Figures 1D and 1E). We found that the glucose-dependent reduction in hypocotyl elongation observed in the wild type is enhanced to a similar extent in etiolated seedlings of the *sr45-1*, *sr45-1 hxk1-1* and *sr45-1 hxk1-2* genotypes (Figures 1D and 1E). These glucose-induced phenotypes are not due to osmotic effects, as they were not observed when equimolar concentrations of sorbitol were used (see Supplemental Figure 2A).

Thus, the *sr45-1 hxk1* double mutants retain full hypersensitivity to glucose both at the level of cotyledon development and hypocotyl elongation in the dark, suggesting a HXK1-independent role of the SR45 splicing factor in sugar signaling. Alternatively, HXK1 and SR45 could act in a single pathway, with the former controlling sugar responses exclusively by downregulating the latter. This possibility appeared less likely as *HXK1* disruption does not affect *SR45* expression, at least at the mRNA level (see Supplemental

Figure 3), and stable overexpression of high *SR45* levels in transgenic *Arabidopsis* plants (see Supplemental Figure 4A) had no effect on the sugar response (see Supplemental Figures 4B and 4C).

Disruption of SnRK1.1 Signaling Attenuates Glucose Hypersensitivity Caused by Loss of *SR45* Function

We then looked into alternative components governing the mode of action of the SR45 splicing factor in sugar responses. We focused on the SnRK1 protein kinase, a central integrator for stress and energy signaling (Baena-Gonzalez et al., 2007), also because overexpression of the SnRK1.1 catalytic subunit in *Arabidopsis* results in hypersensitivity to both glucose and ABA during early seedling development (Jossier et al., 2009; Tsai and Gazzarrini, 2012), a strikingly similar phenotype to that caused by loss of *SR45* function (Carvalho et al., 2010).

We started by analyzing the expression and splicing pattern of *SnRK1.1* in the *sr45-1* mutant background. According to the current annotation (TAIR10; www.arabidopsis.org), the *SnRK1.1* gene encodes three mRNAs arising from alternative selection of 5' splice sites in its first intron (see Supplemental Figure 5A). Using real-time RT-qPCR analyses to detect total *SnRK1.1* expression, we found no significant differences between wild-type and mutant plants under control or glucose-fed conditions (Figure 2A). Furthermore, semi-quantitative RT-PCR analysis using primers designed to detect all three transcripts allowed significant amplification of only the first splice variant, *SnRK1.1.1*, which appeared highly and similarly expressed in both genotypes in the presence or absence of glucose (see Supplemental Figure 5B, upper panel). Primers designed to amplify exclusively the other two alternative transcripts enabled detection of the *SnRK1.1.2* and *SnRK1.1.3* splice variants, which were also expressed at similar levels in all samples analyzed (see Supplemental Figure 5B, middle panel). Thus, at least under the conditions tested, *SnRK1.1.1* is the most highly expressed *SnRK1.1* mRNA, with our results revealing no SR45-dependent changes in the expression or splicing pattern of the *SnRK1.1* gene.

We next used epistatic analysis to evaluate whether the function of SR45 in glucose responses is affected by the SnRK1.1 kinase. To perform genetic crosses with the *sr45-1* mutant, we used a homozygous insertion line for the *SnRK1.1* gene, *snrk1.1-3*, which is

disrupted just before the gene's last exon (Mair et al., 2015). RT-PCR analysis using primers flanking the T-DNA segment did not amplify any of the *SnRK1.1* transcripts (see Supplemental Figure 1B), confirming that *snrk1.1-3* is a true loss-of-function mutant. As seen in Figures 2B to 2E, we found that *snrk1.1-3* seedlings display reduced sensitivity to glucose during early development. In fact, the presence of high glucose concentrations (4% and 5%) in the growth medium led to a slight but evident decrease in cotyledon greening of wild-type seedlings, but did not affect greening of *snrk1.1-3* cotyledons (Figures 2B and 2C). Moreover, though etiolated *snrk1.1-3* seedlings grown in the absence of exogenous glucose displayed shortened hypocotyls, increasing concentrations of the sugar exerted a stronger inhibitory effect on the elongation of wild-type hypocotyls than on those of the *snrk1.1-3* mutant (Figures 2D and 2E).

Importantly, we found that the sugar oversensitivity exhibited by the *sr45-1* mutant is markedly attenuated by disruption of the *SnRK1.1* gene. Indeed, the strong impairment of cotyledon development displayed by *sr45-1* seedlings under moderate to high concentrations of glucose (3% and 4%) is largely restored in the *sr45-1 snrk1.1-3* double mutant (Figures 2B and 2C). Furthermore, glucose inhibition of hypocotyl elongation in dark-grown *sr45-1 snrk1.1-3* seedlings is substantially less pronounced than in the *sr45-1* mutant (Figures 2D and 2E). Again these effects are sugar-specific, as they were not evident in equivalent concentrations of sorbitol (see Supplemental Figure 2B).

In conclusion, regarding both cotyledon development and hypocotyl elongation in the dark, the glucose phenotype of the *sr45-1 snrk1.1-3* double mutant was intermediate between that exhibited by the wild type and the *sr45-1* mutant. These findings could indicate either that the two components act independently to affect the same sugar responses during early seedling development, or that the function of SR45 in sugar signaling is largely dependent on the SnRK1 energy sensor.

SR45 Modulates SnRK1.1 Protein Levels Under Glucose Conditions

To further investigate a potential link between the SR45 splicing factor and the SnRK1.1 protein kinase in sugar signaling, and given that the *SnRK1.1* pre-mRNA does not appear to be a molecular target of SR45 (see Figure 2A and Supplemental Figure 5), we then

used specific antibodies to examine the levels of the SnRK1.1 protein in the *sr45-1* mutant background.

Remarkably, despite unchanged *SnRK1.1* transcript levels in *sr45-1*, but consistent with the fact that transgenic *Arabidopsis* plants with enhanced SnRK1.1 levels phenocopy the *sr45-1* loss-of-function mutant (Jossier et al., 2009; Tsai and Gazzarrini, 2012), western blotting analysis indicated that *sr45-1* contains significantly higher amounts of the SnRK1.1 protein kinase than the wild type, particularly in the presence of glucose (Figure 3A). No evident difference in the amounts of SnRK1.1 in wild-type and mutant plants was observed when both genotypes were treated with equimolar concentrations of sorbitol (see Supplemental Figure 6), showing that the effect of the *sr45-1* mutation on SnRK1.1 levels is glucose-specific and not solely due to the osmotic stress imposed by the sugar.

In agreement with enhanced SnRK1.1 protein levels in the glucose-treated *sr45-1* mutant, genes whose transcription is activated by SnRK1.1, such as *DARK-INDUCED 6* (*DIN6*, also known as *GLUTAMINE-DEPENDENT ASPARAGINE SYNTHETASE 1, ASN1*), *DARK-INDUCED 1 (DIN1* also known as *SENESCENT 1* or *SENESCENCE-ASSOCIATED GENE 1*, *SEN1*) and *DRM2* (*DORMANCY-ASSOCIATED GENE 2*), appear markedly overexpressed in *sr45-1* under glucose conditions (Figure 3B). By contrast, the expression of photosynthesis-related genes, such as *CHLOROPHYLL A/B BINDING PROTEIN 1* (*CAB1*) and *RIBULOSE BISPHOSPHATE CARBOXYLASE (RUBISCO) SMALL SUBUNIT 3B* (*RBCS3B*), which are typically associated with HXK1-mediated signaling (Jang and Sheen, 1994; Xiao et al., 2000), was not significantly changed in the glucose-fed *sr45-1* mutant (see Supplemental Figure 7).

Taken together, the above results favored the hypothesis that SR45 controls sugar responses by affecting the SnRK1.1 pathway rather than via HXK1 signaling.

SR45 Affects Alternative Splicing of Many *Arabidopsis* Genes

In an attempt to identify endogenous splicing targets of SR45 that could underly its role in sugar signaling, we used a custom high-resolution RT-PCR panel (Simpson et al., 2008) to compare multiple alternative splicing events in wild-type and *sr45-1* mutant seedlings grown in the absence or presence of 3% glucose. The panel included 242 *Arabidopsis* genes (see Supplemental Table 1), encoding transcription factors (85), proteins involved in

RNA binding and processing (55), protein kinases and phosphatases (28), microRNAs (2), as well as other miscellaneous proteins (72). Of the 501 alternative splicing events analyzed in these genes, 184 and 83 involve the alternative selection of 3' and 5' splice sites, respectively, 47 and 21 represent intron retention and exon skipping events, while 166 events are still to be defined. Among the 242 genes analyzed, 93 displayed significant changes (> 3%, P < 0.05) in the ratios of alternatively-spliced transcripts between wild-type and *sr45-1* plants grown under control conditions (see Supplemental Table 2), while in the presence of glucose only 67 genes were found to display significant alternative splicing changes (> 3%, P < 0.05) (see Supplemental Table 3). The alternative splicing of 53 genes was affected by the *sr45-1* mutation in both control and glucose conditions. Importantly, and in agreement with our analysis of the splicing pattern of the *SnRK1.1* gene (see Supplemental Figure 5), no significant changes were observed in the relative abundance of the two alternative *SnRK1.1*-specific transcripts analyzed by the panel under either control or glucose conditions.

We also asked whether the SR45 protein would preferentially affect splicing of genes involved in specific functions or a particular type of alternative splicing event. To address this question, we compared the functional classification and alternative splicing event distribution profiles for the total of genes included in the RT-PCR panel with those for the set of genes showing *sr45-1*-induced splicing changes either under control or glucose conditions (Figure 4). Although the small sample size did not allow detection of statistically significant differences between functional category distribution profiles ($P > 0.05$, Fisher's exact test with Bonferroni correction for multiple testing), our data suggest that particularly under glucose conditions SR45 targets predominantly the splicing of genes encoding RNA-binding and processing proteins at the expense of transcription factors (Figure 4A). Strikingly, among the splicing-related genes significantly affected by the *sr45-1* mutation, nine encode SR or SR-like proteins: *SR34*, *SR34a*, *SR34b*, *SCL30a*, *RS2Z32*, *RS2Z33*, *RS31*, *RS40*, and *SR45a* (see Supplemental Tables 2 and 3). Regarding the alternative splicing type distribution profile (Figure 4B), the only statistically significant difference detected was a decline in undefined events in control conditions ($P < 0.05$, Fisher's exact test with Bonferroni correction for multiple testing), under which the *sr45-1* mutation appears to favor the selection of alternative 3' splice sites, followed by alternative 5' splice

sites and exon skipping events, whereas in the presence of glucose a slight bias for intron retention and exon skipping is apparent.

Of the genes whose splicing was altered in *sr45-1* seedlings grown in glucose, only four (highlighted in white in Supplemental Table 3) exhibited substantial changes (≥ 20%) in the ratio of their splice variants — a CC1-like splicing factor, a cysteine-rich receptor-like kinase (*CRK18*), a P-loop containing hydrolase and a Pinin domain protein of unknown function. As seen in Supplemental Figure 8A, loss of *SR45* function altered 5' and 3' splice site selection in the fourth intron of the CC1-like splicing factor gene, favoring the expression of at least two splice variants harboring premature termination codons (PTCs). The *sr45-1* mutation also promoted an intron retention event in the pre-mRNA encoding the CRK18 receptor-like kinase (see Supplemental Figure 8B). In the two other genes, encoding the nucleoside triphosphate hydrolase or the Pinin domain protein, SR45 function controlled only 3' or both 5' and 3' splice site choice, respectively (see Supplemental Figures 8C and 8D). Noticeably, while the alternative splicing changes in the genes encoding the hydrolase and the Pinin protein were also striking (≥ 20%) under control conditions, the effect of the mutation on splicing was less evident for the CC1-like splicing factor and non detectable for the *CRK18* receptor-like kinase in the absence of glucose (see Supplemental Figure 8 and Supplemental Tables 2 and 3). As they are as yet not functionally characterized, whether any of these *Arabidopsis* genes plays a role in sugar signaling is unknown. Nevertheless, these findings clearly indicate that the SR45 protein controls alternative splicing of several in vivo mRNA targets in a glucose-dependent manner.

The *sr45-1* Mutation Affects Alternative Splicing of the *SR45* Pre-mRNA

Interestingly, results from the high-resolution RT-PCR panel analysis also revealed that the splicing pattern of the *SR45* gene is altered in the *sr45-1* mutant. This loss-of-function mutant harbors a T-DNA insertion in the seventh exon of the *SR45* mRNA and has been reported to express a truncated transcript upstream of the insertion, albeit at substantially lower levels than the wild-type full-length mRNA (Ali et al., 2007). Selection of an alternative 3' splice site in intron 6 generates two *SR45* transcripts that differ by 21 nucleotides (Palusa et al., 2007; Zhang and Mount, 2009). As the *SR45*-specific primer

pair used in the RT-PCR panel is located upstream of the T-DNA insertion site and flanks the alternative 3' splice sites (Figure 5A), we were able to analyze the effects of the *sr45-1* mutation on the proportion of the two *SR45* splice variants.

As shown in Figure 5B, the level of the first splice variant, *SR45.1*, relative to *SR45.2* was lower in the *sr45-1* mutant than in the wild type (see also Supplemental Table 2), with the effect of the mutation being further enhanced by the presence of glucose (see also Supplemental Table 3). Although the possibility of a *cis* effect arising from the close proximity of the T-DNA insertion cannot be excluded, these data suggest that alternative splicing of the *SR45* gene is under either direct or indirect control of the splicing factor it encodes, which appears to promote proximal 3' splice site usage in intron 6 of its pre-mRNA, particularly in the absence of glucose.

SR45 Promotes SnRK1.1 Proteasomal Degradation

Given that no evident candidates for molecular SR45 targets controlling sugar signaling were retrieved from the alternative splicing RT-PCR panel, and to gain insight into the mechanisms governing the mode of action of the SR45 splicing factor, we next investigated whether the elevated levels of SnRK1.1 detected in the *sr45-1* mutant were a result of enhanced protein biosynthesis or reduced proteolysis.

As shown in Figure 6, the difference in SnRK1.1 amounts between mutant and wild type observed under glucose conditions was also evident in the presence of the protein synthesis inhibitor cycloheximide (CHX). By contrast, treatment with MG132, a potent proteasomal inhibitor, resulted in a more significant increase in SnRK1.1 levels in wild-type plants than in the *sr45-1* background, supressing the difference in SnRK1.1 content between the two genotypes (Figure 6).

These results strongly suggest a role for SR45 in destabilizing the SnRK1.1 protein in response to sugars. Thus, the SR45 splicing factor appears to act through glucose-responsive modulation of the degradation of a conserved protein kinase known to sense stress-associated energy-deprivation and coordinate sugar and ABA responses (Baena-Gonzalez et al., 2007; Rodrigues et al., 2013).

SR45 Targets Alternative Splicing of the *5PTase13* Gene Encoding an Inositol 5-Phosphatase Implicated in SnRK1.1 Protein Degradation

Two components have previously been implicated in the regulation of the stability of the SnRK1 protein kinase. Pleiotropic regulatory locus 1 (PRL1), a nuclear WD40 repeat protein that binds SnRK1 inhibiting its protein kinase activity in vitro (Bhalerao et al., 1999), has been suggested to act as the substrate receptor for the degradation of SnRK1.1 by a cullin 4 E3 ligase in *Arabidopsis* (Lee et al., 2008). On the other hand, a *myo*-inositol polyphosphate 5-phoshatase, 5PTase13, was also found to interact via its WD40 domain with SnRK1.1 and to modulate the amounts of this protein that are targeted to proteasomal degradation (Ananieva et al., 2008). Thus, the transcripts encoding these two *Arabidopsis* WD proteins represented prime candidates for functional targets of the SR45 splicing factor.

The current genome annotation indicates that the *PRL1* gene produces a single mRNA, whose expression we found to be unaltered in the *sr45-1* mutant (data not shown). On the other hand, by cloning and sequencing the corresponding cDNAs, we confirmed expression of the two currently annotated (TAIR10; www.arabidopsis.org) *5PTase13* splice variants. While *5PTase13.2* derives from constitutive splicing of the pre-mRNA, retention of the 102-bp intron 6 gives rise to a longer alternative transcript, *5PTase13.1* (Figure 7A). As this alternatively-spliced fragment is in frame, the two predicted 5PTase13 splice forms differ only in 34 amino acids, which include no recognizable motif but lie within the catalytic domain of the protein (Zhong and Ye, 2004).

Importantly, although no significant differences in total gene expression were observed, we found that the splicing pattern of the *5PTase13* gene is markedly altered in the *sr45-1* mutant. As seen in Figure 7B, semi-quantitative RT-PCR analysis in glucose-treated leaves using primers designed to detect both *5PTase13* splice variants simultaneously indicated that the abundance of the longer *5PTase13.1* transcript is considerably higher in the mutant. Real-time RT-qPCR analysis confirmed that while total *5PTase13* gene expression is unaltered in *sr45-1*, *5PTase13.1* levels in the mutant are increased almost two fold during exposure to glucose (Figure 7C, upper panel). Consequently, as also seen in Figure 7C (lower panel), the proportion of the *5PTase13.1* transcript is significantly higher in *sr45-1* under glucose conditions, indicating that loss of *SR45* function results in enhanced retention of a short intron in the *5PTase*13 mRNA.

It is interesting to note that the *5PTase13* sequence that is alternatively spliced fits the recent definition of an exitron (Marquez et al., 2015) and appears to be conserved at the protein level across eudicotyledons. Remarkably, this exitron's 3' splice site contains an RNA motif highly similar to the M3 *cis*-element found by Xing et al. (2015) to be overrepresented in SR45-associated transcripts.

These results clearly show that the SR45 protein is required for accurate splicing of the pre-mRNA encoding an inositol 5-phosphatase previously implicated in the regulation of SnRK1.1 protein stability (Ananieva et al., 2008), thus providing a link between SR45 function and the modulation of SnRK1.1 levels in response to sugars.

DISCUSSION

We have previously shown that the *Arabidopsis sr45-1* mutant, initially described to display pleiotropic developmental defects under normal growth conditions (Ali et al., 2007), is impaired in glucose and ABA signaling during early seedling development (Carvalho et al., 2010). In the present report, we first asked whether control of glucose responses by the SR45 RNA-binding protein would depend on HXK1, an evolutionarily conserved sugar sensor that integrates nutrient and hormone signals to regulate gene expression and plant growth and development (Moore et al., 2003). Our results showed that steady-state *HXK1* transcript levels are unaffected by loss of *SR45* function and, most importantly, that the glucose hypersensitivity of the *sr45-1* mutant is unaltered in the absence of *HXK1* expression. This could indicate that the two components function in the same linear pathway, with the HXK1 sugar kinase ultimately acting in early growth glucose responses by inhibiting the SR45 splicing factor. However, because our data also indicated on one hand that expression of the *SR45* gene is unaffected by loss of *HXK1* function and on the other that its overexpression in transgenic seedlings has no effect on the response to glucose, we favored the alternative possibility that the proteins encoded by these two genes operate in distinct pathways.

We thus turned our attention to the SnRK1 subfamily of plant protein kinases, which are activated by stress-associated energy deprivation and, as their orthologs SNF1 in yeast and AMPK in mammals, appear to act as regulators of metabolism. In line with this, *SnRK1.1* silencing lines utilize exogenously supplied sucrose more efficiently than the wild

type (Baena-Gonzalez et al., 2007), and our phenotypic analysis of a *SnRK1.1* loss-of-function allele revealed slight insensitivity to glucose during early plant growth. Furthermore, our epistatic analyses showed that *SnRK1.1* inactivation in the *sr45-1* background largely rescues the mutant's glucose hypersensitive phenotypes during early seedling development. The fact that these phenotypes are not fully suppressed, despite *snrk1.1-3* being a true null allele (reported also by Mair et al., 2015), points to the contribution of other components to SR45 control of sugar signaling. Nevertheless, our results clearly implicate SnRK1 in this process and suggest that the SR45 splicing factor could rely on a functional SnRK1 protein kinase for its negative regulation of plant sugar responses. Remarkably, and despite our finding that SR45 does not affect expression or splicing of the *SnRK1.1* gene, we found that, particularly in the presence of glucose, the *sr45-1* mutant contains significantly higher amounts of SnRK1.1 protein than the wild type. In agreement with this, under glucose conditions, marker genes for SnRK1.1 activity are clearly upregulated in the *sr45-1* background. By contrast, it is interesting to note that the expression of photosynthesis-related genes that have been implicated in HXK1 signaling was not significantly altered.

As *SnRK1.1* overexpression has been previously reported to confer oversensitivity to sugars and ABA during early seedling development (Jossier et al., 2009; Tsai and Gazzarrini, 2012), the enhanced SnRK1.1 levels alone could explain both the glucose- and ABA-related phenotypes exhibited by the *sr45-1* mutant. In fact, a molecular link between ABA and sugar signal transduction has been uncovered, where ABA induces SnRK1 signaling through the inhibition of two established repressors of the ABA pathway, ABI1 and PP2CA (Rodrigues et al., 2013). The *sr45-1* mutant shows enhanced ability to accumulate ABA in response to glucose (Carvalho et al., 2010), while *35S:SnRK1.1* transgenic lines are reportedly unaffected in their ABA content at least under control conditions (Jossier et al., 2009). Nevertheless, decreased ABA levels have been found in SnRK1-deficient pea (*Pisum sativum*) antisense lines (Radchuk et al., 2010), which exhibit an ABA-insensitive-like phenotype (Radchuk et al., 2006). In *Arabidopsis*, the enhanced glucose and ABA sensitivity displayed by both the *sr45-1* mutant and SnRK1.1 overexpressor plants is observed as a postgermination growth arrest, which functions as a developmental checkpoint to monitor adverse environmental conditions in the transition

462 from hetero- to autotrophic growth (Lopez-Molina et al., 2001). Jossier et al. (2009) have
463 proposed that the SnRK1 protein kinase contributes to regulate ABA-sugar interactions
464 during this transition.
465 Although activation of SnRK1 signaling is similarly inhibited by glucose and sucrose
466 (Baena-Gonzalez et al., 2007; Baena-Gonzalez and Sheen, 2008), sucrose is known to
467 exert signaling functions independently of its degradation products (Ruan, 2014), and
468 some studies have reported sucrose-specific effects on SnRK1 (Purcell et al., 1998;
469 Bhalerao et al., 1999; Tiessen et al., 2003; McKibbin et al., 2006). The *sr45-1* mutant is
470 hypersensitive to both glucose and sucrose (Carvalho et al., 2010) and SnRK1.1
471 overexpressors are also hypersensitive to both sugars (Baena-Gonzalez et al., 2007;
472 Rodrigues et al., 2013). The results presented here indicate that the glucose
473 hypersensitivity of *sr45-1* is partly dependent on SnRK1, but whether this is the case also
474 for sucrose remains to be confirmed.
475 To search for mRNA targets that could link SR45 function to SnRK1 signaling, we
476 compared multiple alternative splicing events in wild-type and *sr45-1* mutant seedlings.
477 Although no obvious candidates were identified, the results from the alternative splicing
478 RT-PCR panel provided important information on the mode of action of the SR45 protein.
479 Firstly, out of the 242 *Arabidopsis* genes analyzed, 107 (~44%) were found to have their
480 splicing pattern changed by loss of *SR45* function, substantiating a broad role for this SR-
481 related protein in regulating alternative splicing in vivo. Secondly, as reported for other
482 plant and animal SR-related splicing factors (Lopato et al., 1999; Kalyna et al., 2003;
483 Sanford et al., 2009; Anko et al., 2012), SR45 appears to target preferentially genes
484 encoding other RNA binding and processing factors, pointing to an even broader influence
485 of SR45 on posttranscriptional control of in vivo gene expression. In particular, the *sr45-1*
486 mutation significantly affected the splicing pattern of nine *Arabidopsis* SR or SR-like
487 genes, uncovering another six SR45 SR targets in addition to those reported by Ali et al.
488 (2007). At least eight out of these nine SR mRNAs are likely to represent direct targets of
489 the SR45 protein, as they were recently found associated with the splicing factor in vivo
490 (Xing et al., 2015). Thirdly, loss of *SR45* function seems to affect preferentially 5' and 3'
491 splice site selection. This is in line with the model proposed by Day et al. (2012), where
492 SR45 regulates alternative splicing of the *SR30* gene by recruiting core spliceosomal

493 components to 5’ and 3’ splice sites. Interestingly, when the *sr45-1* mutant is grown in the
494 presence of glucose, the alternative splicing event distribution appears to be directed
495 towards intron retention and exon skipping. Fourthly, because the *sr45-1* allele expresses
496 truncated transcripts upstream of the T-DNA insertion, we were able to detect changes in
497 the selection of alternative 3’ splice sites in the sixth intron, suggesting that SR45
498 regulates splicing of its own pre-mRNA. This is in agreement with a recent report where
499 the *SR45* mRNA was found bound to SR45 complexes immunoprecipitated from
500 transgenic *Arabidopsis* plants (Xing et al., 2015). Autoregulation of alternative splicing by
501 SR and other splicing-related proteins has been reported in many systems, including for
502 the *Arabidopsis* SR30 (Lopato et al., 1999), RS2Z33 (Kalyna et al., 2003) and SCL33
503 (Thomas et al., 2012) SR proteins. Lastly, results from the RT-PCR panel indicate that the
504 splicing activity of the SR45 RNA-binding protein is sugar-responsive, as 14 genes were
505 only affected by the *sr45-1* mutation under glucose conditions. Of these, one as yet
506 uncharacterized gene, *CRK18*, encoding a cysteine-rich receptor-like kinase, showed
507 extensive *sr45-1*-induced changes in its splicing pattern and represents a prime candidate
508 for a role in SR45-related sugar responses.
509 In the face of the evidence pointing to a role for SnRK1.1 in mediating SR45 sugar
510 functions, we next addressed the mechanisms underlying SR45 control of SnRK1.1 levels.
511 Importantly, our results indicated that the enhanced SnRK1.1 levels observed in the *sr45-1*
512 mutant are not a result of higher protein synthesis rates but rather of reduced proteasomal
513 degradation of the protein kinase. In animal systems, at least two splicing factors have
514 been implicated in the regulation of posttranslational modifications that act as signals for
515 proteasomal degradation. The U2AF65 essential splicing factor was shown to stabilize the
516 TRF1 protein, a negative regulator of telomere length, by inhibiting its ubiquitin-dependent
517 degradation (Kim and Chung, 2014), while the human SR protein SF2/ASF stimulates
518 sumoylation both in vivo and in vitro, with its depletion inhibiting overall SUMO conjugation
519 (Pelisch et al., 2010). Interestingly, sumoylation was recently shown to be important for
520 controlling SnRK1 complex stability, establishing a connection between SnRK1 activity
521 and its proteasomal degradation (Crozet et al., 2016). Although a direct effect of SR45 on
522 SnRK1 degradation through a splicing-unrelated function cannot be excluded, our finding
523 that the SR45 protein is required for efficient processing of the sixth intron of the

5PTase13 gene specifically under glucose-fed conditions provides a mechanistic link between the function of the RNA-binding protein in sugar responses and its glucose-responsive modulation of SnRK1 protein levels.

The *Arabidopsis 5PTase13* gene encodes a *myo*-inositol polyphosphate 5-phosphatase that acts as a positive regulator of SnRK1.1 activity under low-nutrient or sugar-stress conditions by reducing the amounts of SnRK1.1 protein targeted to the proteasome (Ananieva et al., 2008). Consistent with the 5PTase13 protein promoting SnRK1.1 activity at high glucose concentrations, mutations in the *5PTase13* locus lead to the opposite phenotype conferred by gain of *SnRK1.1* and loss of *SR45* function — insensitivity to both sugar and ABA during early seedling development. Given the described role of this inositol phosphatase in stabilizing the SnRK1.1 kinase (Ananieva et al., 2008), we propose that SR45 regulates SnRK1.1 levels in response to sugars by modulating alternative splicing of the *5PTase13* gene (Figure 8). Indeed, our results suggest that, without changes in total gene expression levels, a shift in *5PTase13* pre-mRNA splicing from the fully-spliced variant to a longer transcript retaining the in-frame intron 6 leads to stabilization of the SnRK1.1 protein. In fact, the location of the 34-amino acid stretch introduced by this intron retention event raises the possibility that it affects the catalytic activity of the 5PTase13 phosphatase. SR45 could regulate alternative splicing of the *5PTase13* pre-mRNA through direct binding to intron 6 and subsequent modulation of splice site choice by interaction with the U1-70K and U2AF^{35} spliceosomal components, two reported SR45 binding partners (Golovkin and Reddy, 1999; Ali et al., 2008; Day et al., 2012) that recognize 5' and 3' splice sites, respectively (Zhuang and Weiner, 1986; Kohtz et al., 1994; Wu et al., 1999; Wahl et al., 2009). Alternatively, SR45 could control *5PTase13* splicing indirectly, e.g. via regulation of processing of (an) established direct SR protein gene target(s). In a recent study, and despite the presence of a *cis*-element overrepresented in SR45-associated RNAs, Reddy and co-workers found no *5PTase13* mRNA associated with GFP-tagged SR45 precipitated from *Arabidopsis* seedlings grown in liquid culture (Xing et al., 2015). However, our data indicate that SR45 regulates retention of the *5PTase13* intron exclusively under sugar conditions, and RIP-seq assays from glucose-treated SR45-tagged transgenic plants will be required to discern whether *5PTase13* is a direct in vivo target of the RNA-binding protein. Future functional characterization of the individual

5PTase13 splice variants should also conclusively establish both their differential roles in the regulation of SnRK1 stability and their ability to modulate the *sr45-1* sugar phenotype, thus verifying the *5PTase13* pre-mRNA as a functional target of the SR45 splicing factor. In any case, the evidence presented here corroborates a SnRK1-mediated mechanism for SR45 control of sugar responses and clearly defines this RNA-binding protein as a novel regulator of SnRK1 signaling in *Arabidopsis*.

METHODS

Plant Materials and Growth Conditions

The *Arabidopsis thaliana* Colombia (Col-0) ecotype was used as the wild type in all experiments. A homozygous line for the *sr45-1* mutant (SALK_004132) was previously isolated by Carvalho et al. (2010), and seeds homozygous for T-DNA insertions within the *HXK1* locus, *hxk1-1* (SALK_018086) and *hxk1-2* (SALK_070739), were kindly provided by S. Yanagisawa (University of Tokyo, Japan). The *snrk1.1-3* (GK-579E09) homozygous line has been previously described by Mair et al. (2015). The *sr45-1 hxk1-1*, *sr45-1 hxk1-2* and *sr45-1 snrk1.1-3* double mutants were generated through genetic crossing of the respective single mutant lines, with F_2 plants homozygous for T-DNA insertions in both the *HXK1* and the *SR45* or the *SnRK1.1* and the *SR45* loci being selected by PCR genotyping using *HXK1*- or *SnRK1.1*- and *SR45*-specific primers (see Supplemental Table 4), and primers annealing at the left border of the T-DNA.

To generate transgenic *Arabidopsis SR45* overexpressor lines, the *SR45.1* coding sequence was PCR-amplified (see Supplemental Table 4), using cDNA extracted from 4-week-old seedlings as a template, and inserted under the control of the 35S promoter into the GFP-tagged version of the binary pBA002 vector via the *Xho*I/*Pac*I restriction sites. Two transgenic lines displaying significant *SR45.1* overexpression (see Supplemental Figure 4A) were recovered upon agrotransformation of wild-type (Col-0) *Arabidopsis* plants with the resulting construct, and phenotypic analyses were conducted in T3 plants.

Seeds were surface sterilized and sown on MS medium containing 1X Murashige and Skoog (MS) salts (Duchefa Biochemie), 2.5 mM MES (pH 5.7), 0.5 mM *myo*-inositol and 0.8% agar. After stratification for 3 d in the dark at 4ºC, seeds were placed in a growth

chamber under 16-h photoperiod (90 µmol m^{-2} s^{-1} white light) at 22ºC (light period)/18ºC (dark period) and 60% relative humidity (RH). After 2-3 weeks, seedlings were transferred to soil in individual pots.

Glucose Assays

Seeds were surface sterilized and water imbibed in the dark for 3 d at 4ºC. After stratification, 80 to 100 seeds of each genotype were sown in triplicate on MS medium supplemented or not with the appropriate concentrations of D-glucose (Sigma) or D-sorbitol (VWR International), before transfer to the growth chamber (16-h photoperiod). After 7 d, cotyledon greening rates were calculated as the number of seedlings exhibiting green color over the total of germinated (displaying radicle emergence) seeds. For assessment of hypocotyl elongation, 30 to 100 seeds of each genotype were surface sterilized and stratified as described above, plated on MS plates supplemented or not with the appropriate concentrations of D-glucose or D-sorbitol and grown vertically under complete darkness at 22ºC for 7 d. Etiolated seedlings were illuminated for 12 h before hypocotyl length measurements using the NIH ImageJ software (http://rsbweb.nih.gov/ij).

For transient glucose assays in leaves, seeds were directly sown in soil after stratification and pots placed in a growth chamber under a 12-h photoperiod (100 µmol m^{-2} s^{-1} white light) at 22ºC (light period)/18ºC (dark period) and 60% RH. Leaf disks from 5/6-week old plants were immersed in water (control conditions), 1.5% D-glucose or 1.5% D-sorbitol (VWR International) and incubated in the light (except when otherwise indicated). The plant material was collected after 6 h for RNA or protein extraction. To inhibit protein synthesis or proteasomal degradation, respectively 100 µM cycloheximide (Sigma) or 50 µM MG132 (Calbiochem) were added 1 h prior to the onset of the glucose treatment.

RNA Extraction and Gene Expression Analyses

Total RNA was extracted from whole *Arabidopsis* seedlings using the innuPREP Plant RNA kit (Analytik Jena BioSolutions) and from leaves using TriReagent (Sigma) following the manufacturers' protocols. All RNA samples were digested with DNAseI (Promega) and phenol-chloroform purified before reverse transcription (RT) with M-MLV reverse transcriptase (Promega) and a poly-T primer.

Real-time RT-qPCR was performed using a CFX 384 Touch Real-Time PCR Detection System (Bio-Rad) and the Absolute SYBR Green ROX Mix (Thermo Scientific) on 2.5 µL of cDNA (diluted 1:10) per 10 µL of reaction volume, containing 300 nM of each gene-specific primer (see Supplemental Table 4). Specificity of the amplified products was confirmed by a melting curve step. For each condition tested, two independent biological and technical repetitions were performed as described by Remy et al. (2014). Data were processed using Q-Gene (Muller et al., 2002) that took the respective primer efficiency into consideration.

For semi-quantitative RT-PCR, preliminary PCRs using the various gene-specific primers (see Supplemental Table 4) were carried out with different cycles to determine the linear range of amplification. Based on these analyses, 20 to 35 cycles were chosen for cDNA detection, depending on the gene (see Supplemental Table 4). Amplified DNA fragments were separated in 1% agarose gels. Each RT-PCR experiment was repeated independently at least three times to verify the observed changes in gene expression.

High-Resolution Alternative Splicing RT-PCR panel

Wild-type (Col-0) and *sr45-1* mutant seedlings were grown in MS plates supplemented or not with 3% glucose and the plant material harvested at the same developmental stage (approximately 50% cotyledon expansion). Total RNA was extracted using the RNeasy Plant Mini Kit (Qiagen). High-resolution RT-PCR experiments were performed after DNase I (RNase-free DNase set, Qiagen) treatment according to the manufacturer's instructions and first-strand cDNA synthesis on 5 µg of total RNA using "Ready-to-go you-prime" first strand beads (GE-Healthcare) and 0.5 µg of oligo $d(T)^{18}$ (Invitrogen). The RT reaction was diluted to a final volume of 100 µL, and 1 µL was aliquoted into a 96-well reaction plate along with 2.5 µL 10X PCR buffer (100 mM Tris-HCl, 15 mM $MgCl_2$, 500 mM KCl, pH 8.3) (Roche), 4 µl of 1.25 mM dNTPs (Promega), 1 µl of 10 µM stock of each of the alternative splicing event-specific primers and 0.125 µl of Taq DNA polymerase (5 U/µl) (Roche) to give a final volume of 25 µl, with a standard PCR reaction being performed at 24 cycles. This number of PCR cycles was previously shown to be in the linear range of amplification for mRNA transcripts of numerous genes (Simpson et al., 2008). Primers were selected to amplify the expected alternatively-spliced transcripts and yield RT-PCR products of sizes

643 between 70 and 700bp. In order to visualize the RT-PCR products, the forward primer was
644 labeled with 6-Carboxyfluorescein (6-FAM) dye. Primer sequences are given in
645 Supplemental Table 5.
646 Labeled product (1 µL) from the RT-PCR reactions was mixed with 8.95 µL Hi Di
647 Formamide (Applied Biosystems) and with 0.05 µL of GeneScan 500 LIZ internal size
648 standard (Applied Biosystems). Using an ABI 3730 DNA Analyzer (Applied Biosystems),
649 capillary electrophoresis of the RT-PCR fragments was performed. Product size and peak
650 area data were determined by *Genemapper* software analysis (Applied Biosystems). RT-
651 PCR products were accurately identified with ± 1-nt resolution. The relative fluorescent
652 peak areas for RT-PCR products with expected sizes for the alternatively-spliced products
653 were extracted, and the proportion of the alternatively-spliced products was calculated by
654 dividing the value of each spliced product by the sum of the values of all products. A
655 minimum of three biological repetitions was performed to determine statistically significant
656 changes in alternative splicing under the conditions tested. The mean alternative splicing
657 proportions with standard errors were calculated for the three separate biological
658 repetitions. Pairwise comparisons were made between wild-type and mutant plants grown
659 under control or glucose conditions. Analysis of variance was used to determine significant
660 variation between the means ($P < 0.05$), and only genes displaying a > 3% change in the
661 abundance of at least one of their alternatively-spliced transcripts in each pairwise
662 comparison were selected.
663 The alternative splicing RT-PCR panel included 242 genes predicted to undergo
664 alternative splicing and two controls (see Supplemental Table 1). Genes were selected
665 from annotated events found in different databases — ASIP
666 (http://www.plantgdb.org/ASIP/Enter_DB.php), TIGR (http://compbio.dfci.harvard.edu/cgi-
667 bin/tgi/gimain.pl?gudb=arab), RIKEN (http://rarge.gsc.riken.jp/) and TAIR
668 (http://www.arabidopsis.org/) — and encoded mostly DNA binding proteins and
669 transcription factors, proteins involved in RNA binding and processing, protein
670 kinases/phosphatases and nucleotide binding proteins, as well as other miscellaneous
671 proteins. The primer pairs specific for the two control genes amplified either a
672 constitutively-spliced (At3g12110 — *ACTIN*) or a U12-dependent (At4g02560 —
673 *LUMINIDEPENDENS*) intron.

Protein Extraction and Western Blot Analyses

For total protein extraction, frozen *Arabidopsis* leaves were ground with a mortar and pestle in extraction buffer containing 50 mM Hepes/NaOH (pH 7.5), 1 mM EDTA, 1 mM dithiothreitol and one tablet of the Complete Protease Inhibitor Cocktail (Roche). The homogenates were centrifuged at 18,000*g* (4ºC) and the protein content of the supernatants determined spectrophotometrically at 595 nm using a protein assay kit based on the Bradford method (Bio-Rad) and bovine serum albumin (Sigma) as a standard. Equal amounts of protein were then resolved under reducing conditions in 10% SDS/polyacrylamide gels. Proteins were transferred onto polyvinylidene difluoride (PVDF) membranes (Immobilon-P, Millipore), which were incubated with SnRK1.1 primary antibodies (Agrisera AS10919; diluted 1:500) overnight at 4ºC and then with anti-rabbit peroxidase-conjugated secondary antibodies (Amersham Pharmacia; diluted 1:20,000) for 2 h at room temperature, in TBS buffer (25 mM Tris-HCl pH 7.4, 137 mM NaCl) supplemented with 1% nonfat dry milk. After washing the membranes for 30 min with TBS containing 0.05% Tween 20, membrane-associated peroxidase activity was visualized by enhanced chemiluminescence (ECL). Band intensities were quantified using the NIH ImageJ program (http://rsb.info.nih.gov/ij), with protein levels being normalized to the RuBisCO large subunit band visualized in Ponceau-stained membranes.

Accession Numbers

Arabidopsis Genome Initiative (AGI) locus identifiers for the genes mentioned in this article are as follows: *SR45*, At1g16610; *HXK1*, At4g29130; *SnRK1.1*, At3g01090; *DRM2*, At2g33830; *DIN1*, At4g35770; *DIN6*, At3g47340; CC1-like splicing factor, At5g09880; *CRK18*, At4g23260; P-loop containing nucleoside triphosphate hydrolase, At4g12790; Pinin domain protein, At1g15200; *PRL1*, At4g15900; *5PTase13*, At1g05630; *CAB1*, At1g29930; *RBCS3B*, At5g38410; *ACT2*, At3g18780; *EF1A*, At5g60390; and *SR30*, At1g09140.

Supplemental Data

Supplemental Figure 1. mRNA Analysis of the *SR45, HXK1* and *SnRK1.1* Loss-of-Function Single and Double Mutants Used in This Study.

Supplemental Figure 2. Effect of Sorbitol on Cotyledon Greening and Hypocotyl Elongation. **Supplemental Figure 3.** *SR45* Expression Levels in the *hxk1* Loss-of-Function Mutants.

Supplemental Figure 4. Phenotypic Analysis of *SR45* Overexpressor Lines.

Supplemental Figure 5. Splicing Pattern of the *SnRK1.1* Gene.

Supplemental Figure 6. Effect of Sorbitol on *sr45-1* SnRK1.1 Protein Levels.

Supplemental Figure 7. Effect of *sr45-1* Mutation on Expression of the Photosynthesis-Related *CAB1* and *RBCS3B* Genes.

Supplemental Figure 8. Genes Showing Substantial Alternative Splicing Changes in the *sr45-1* Mutant.

Supplemental Table 1. Genes and Alternative Splicing Events Included in the RT-PCR Panel.

Supplemental Table 2. Genes Showing Significant Alternative Splicing Changes Between Wild-Type and *sr45-1* Seedlings Grown Under Control Conditions.

Supplemental Table 3. Genes Showing Significant Alternative Splicing Changes Between Wild-Type and *sr45-1* Seedlings Grown Under Glucose Conditions.

Supplemental Table 4. Sequences of the Primers Used for RT-PCR Analyses.

Supplemental Table 5. Sequences of the Primers Used to Detect the Alternative Splicing Events Included in the RT-PCR Panel.

ACKNOWLEDGMENTS

We thank S. Yanagisawa for providing the *hxk1* homozygous insertion lines, N.-H. Chua for the pBA002 vector, J. McNicol and D. Faria for help with statistical analysis, V. Nunes and J. Fuller for technical assistance, as well as E. Remy and P. Crozet for critical reading of the manuscript. This work was financed by Fundação para a Ciência e a Tecnologia (Grants PTDC/AGR-PRO/119058/2010 and PTDC/BIA-PLA/3937/2012 awarded to P.D. and E.B.-G. as well as PostDoctoral Fellowships SFRH/BPD/80073/2011 and SFRH/BPD/94796/2013 awarded to R.F.C. and D.S., respectively), the EMBO Installation Program (EMBO-Proj.1984 awarded to E.B.-G.) and funding from the Scottish Government Rural and Environment Science and Analytical Services (RESAS) division (awarded to J.W.S.B. and C.G.S.).

AUTHOR CONTRIBUTIONS

R.F.C., E.B.-G. and P.D. designed the research, R.F.C., D.S. and I.C.R.B. performed the experiments, C.G.S. and J.W.S.B. contributed with new analytical tools, and R.F.C., D.S., C.G.S., J.W.S.B., E.B.-G and P.D. analyzed the data. The article was written by R.F.C. and P.D.

FIGURE LEGENDS

Figure 1. HXK1 Dependency of the *sr45-1* Glucose Phenotypes.

(A) Real-time RT-qPCR analysis of *HXK1* transcript levels in wild-type (Col-0) and *sr45-1* mutant leaves treated or not with 1.5% glucose, using *ACT2* as a reference gene. Results are from two independent experiments and values represent means ± SE (n = 4). Different letters indicate statistically significant differences ($P < 0.05$; Student's t-test).
(B) Representative image of seedlings of the wild type (Col-0), the *sr45-1*, *hxk1-1* and *hxk1-2* single mutants and the *sr45-1 hxk1-1* and *sr45-1 hxk1-2* double mutants, grown in the presence of 4% glucose for 7 d.
(C) Cotyledon greening rates, scored 7 d after stratification, of seedlings of the wild type (Col-0), the *sr45-1*, *hxk1-1* and *hxk1-2* single mutants and the *sr45-1 hxk1-1* and *sr45-1 hxk1-2* double mutants, grown under control conditions or in the presence of 4% glucose (means ± SE, n = 3). Different letters indicate statistically significant differences between genotypes under each condition ($P < 0.05$; Student's t-test).
(D) Representative image of seedlings of the wild type (Col-0), the *sr45-1*, *hxk1-1* and *hxk1-2* single mutants and the *sr45-1 hxk1-1* and *sr45-1 hxk1-2* double mutants, grown in the dark in the presence of 3.5% glucose for 7 d. Bar = 8 mm.
(E) Hypocotyl length, measured 7 d after stratification, of seedlings of the wild type (Col-0), the *sr45-1*, *hxk1-1* and *hxk1-2* single mutants and the *sr45-1 hxk1-1* and *sr45-1 hxk1-2* double mutants, grown in the dark under control conditions or in the presence of 3% or 4% glucose (means ± SE, n = 30-60). Different letters indicate statistically significant differences between genotypes under each condition ($P < 0.05$; Student's t-test).

Figure 2. SnRK1.1 Dependency of the *sr45-1* Glucose Phenotypes.

(A) Real-time RT-qPCR analysis of *SnRK1.1* transcript levels in wild-type (Col-0) and *sr45-1* mutant leaves incubated in the absence or presence of 1.5% glucose, using *ACT2* as a reference gene. Results are from two independent experiments and values represent means ± SE (n = 4). No statistically significant differences between samples were detected ($P > 0.05$; Student's t-test).

(B) Representative image of seedlings of the wild type (Col-0), the *sr45-1* and *snrk1.1-3* single mutants and the *sr45-1 snrk1.1-3* double mutant grown in the presence of 4% glucose for 7 d.

(C) Cotyledon greening rates, scored 7 d after stratification, of seedlings of the wild type (Col-0), the *sr45-1* and *snrk1.1-3* single mutants and the *sr45-1 snrk1.1-3* double mutant, grown under control conditions or in the presence of 3%, 4% or 5% glucose (means ± SE, n = 3). Different letters indicate statistically significant differences between genotypes under each condition ($P < 0.05$; Student's t-test).

(D) Representative image of seedlings of the wild type (Col-0), the *sr45-1* and *snrk1.1-3* single mutants and the *sr45-1 snrk1.1-3* double mutant, grown in the dark in the presence of 3.5% glucose for 7 d. Bar = 10 mm.

(E) Hypocotyl length, measured 7 d after stratification, of seedlings of the wild type (Col-0), the *sr45-1* and *snrk1.1-3* single mutants and the *sr45-1 snrk1.1-3* double mutant, grown in the dark under control conditions or in the presence of 3% or 4% glucose (means ± SE, n = 40-60). Different letters indicate statistically significant differences between genotypes under each condition ($P < 0.05$; Student's t-test).

Figure 3. SR45 Modulation of SnRK1.1 Protein Levels and SnRK1.1-Activated Genes.

(A) Western blotting analysis of SnRK1.1 levels in wild-type (Col-0) and *sr45-1* mutant leaves incubated in the absence or presence of 1.5% glucose. Bands were quantified and relative protein levels determined using the Ponceau loading control as a reference. The blot image is representative of four independent experiments, and the bar graph shows means ± SE of SnRK1.1 protein levels in all assays (n = 4). Different letters indicate statistically significant differences ($P < 0.05$; Student's t-test).

(B) Real-time RT-qPCR analysis of the transcript levels of SnRK1.1 marker genes *DIN6, DIN1* and *DRM2* in wild-type (Col-0) and *sr45-1* mutant leaves incubated in the presence

of 1.5% glucose, using *EF1A* as a reference gene. Results are from two independent experiments and values represent means ± SE (*n* = 4). Asterisks indicate statistically significant differences from the wild type (P < 0.05; Student's *t*-test).

Figure 4. Distribution Profiles for Gene Functional Category and Alternative Splicing (AS) Event of the SR45 Targets Identified by the AS RT-PCR Panel.

(A) Percent functional distribution of the total genes included in the RT-PCR panel and of the genes showing significant AS changes (> 3%, P < 0.05) between wild-type (Col-0) and *sr45-1* mutant seedlings grown under control conditions or in the presence of 3% glucose. Statistical analysis indicated no significant changes between profiles (P > 0.05, Fisher's exact test with Bonferroni correction for multiple testing).

(B) Percent distribution of the different types of AS events among the total AS events analyzed by the RT-PCR panel and the AS events showing significant changes (> 3%, P < 0.05) between wild-type (Col-0) and *sr45-1* mutant seedlings grown under control conditions or in the presence of 3% glucose. The asterisk indicates a significant difference from the total of events in the panel (P < 0.05, Fisher's exact test with Bonferroni correction for multiple testing).

Figure 5. Effect of *sr45-1* Mutation on Alternative Splicing of the *SR45* Pre-mRNA.

(A) Schematic diagram of two splice variants (*SR45.1* and *SR45.2*) produced by the *Arabidopsis SR45* gene. Boxes represent exons with UTRs in black, lines represent introns and the inverted triangle indicates the position of the T-DNA insertion in the *sr45-1* mutant allele. The arrows indicate the location of the primer pair used in the RT-PCR panel, where the sizes of the PCR products obtained for the *SR45.1* and *SR45.2* splice variants were 177 and 156 bp, respectively.

(B) Histogram showing the ratio between the abundance of the *SR45.1* and *SR45.2* splice variants in wild-type (Col-0) and *sr45-1* mutant seedlings grown under control conditions or in the presence of 3% glucose. Different letters indicate statistically significant differences (P < 0.05, Student's *t*-test).

Figure 6. Effect of SR45 on SnRK1.1 Proteasomal Degradation.

Western blotting analysis of SnRK1.1 levels in leaves treated with 1.5% glucose in the absence or presence of 100 μM of the protein synthesis inhibitor cycloheximide (CHX) or of 50 μM of the proteasome inhibitor MG132 (Ponceau-stained membrane is shown as a loading control).

Figure 7. SR45 Regulation of Alternative Splicing of the *5PTase13* Pre-mRNA.

(A) Schematic diagram of two splice variants (*5PTase13.1* and *5PTase13.2*) produced by the *Arabidopsis 5PTase13* gene. Boxes represent exons with UTRs in black, lines represent introns, and arrows indicate the location of the *5PTase13* F1 and R1 primers.
(B) RT-PCR analysis of *5PTase13* transcript levels in wild-type (Col-0) and *sr45-1* mutant leaves incubated in the presence of 1.5% glucose. The location of the F1 and R1 primers used is shown in **(A).** Expression of the *ACT2* gene is shown as a loading control.
(C) Real-time RT-qPCR analysis of total *5PTase13* expression as well as of *5PTase13.1* transcript levels (different Y-axis scales) in wild-type (Col-0) and *sr45*-1 mutant leaves incubated in the absence or presence of 1.5% glucose, using *EF1A* as a reference gene (upper panel). The expression ratio between *5PTase13.1* and total *5PTase13* is also shown (lower panel). Results are from two independent experiments and values represent means ± SE (n = 4). Different letters indicate statistically significant differences ($P < 0.05$; Student's t-test).

Figure 8. Model of SR45-Mediated Sugar Signaling During Early Seedling Development.

High sugars lead to an ABA-mediated early growth arrest in *Arabidopsis*. SR45 negatively regulates sugar signaling by repressing glucose-induced ABA accumulation (Carvalho et al., 2010). One component contributing to SR45 control of sugar signaling is the SnRK1 protein kinase, which is activated by ABA in a PP2C-dependent manner (Rodrigues et al., 2013) and whose overexpression in young *Arabidopsis* seedlings causes glucose and ABA hypersensitivity (Jossier et al., 2009; Tsai and Gazzarrini, 2012). SnRK1 activity is also regulated via SUMOylation/ubiquitination and subsequent degradation by the 26S proteasome (Lee at al., 2008; Crozet et al., 2016). The SR45 SR-like protein regulates SnRK1 protein levels in response to sugars by modulating alternative splicing of the *5PTase13* pre-mRNA — encoding a modulator of SnRK1 proteasomal degradation

847 (Ananieva et al., 2008) — where excision of intron 6 promotes destabilization of the SnRK1
848 protein. Alternatively, SR45 could play a direct role in SnRK1 degradation via a non-
849 splicing function.

850 **REFERENCES**

851 **Aki, T., Konishi, M., Kikuchi, T., Fujimori, T., Yoneyama, T., and Yanagisawa, S.**
852 (2007). Distinct modulations of the hexokinase1-mediated glucose response and
853 hexokinase1-independent processes by HYS1/CPR5 in Arabidopsis. J Exp Bot **58,**
854 3239-3248.

855 **Ali, G.S., and Reddy, A.S.** (2006). ATP, phosphorylation and transcription regulate the
856 mobility of plant splicing factors. J Cell Sci **119,** 3527-3538.

857 **Ali, G.S., Golovkin, M., and Reddy, A.S.** (2003). Nuclear localization and in vivo
858 dynamics of a plant-specific serine/arginine-rich protein. The Plant journal : for cell and
859 molecular biology **36,** 883-893.

860 **Ali, G.S., Prasad, K.V., Hanumappa, M., and Reddy, A.S.** (2008). Analyses of in vivo
861 interaction and mobility of two spliceosomal proteins using FRAP and BiFC. PLoS One
862 **3,** e1953.

863 **Ali, G.S., Palusa, S.G., Golovkin, M., Prasad, J., Manley, J.L., and Reddy, A.S.** (2007).
864 Regulation of plant developmental processes by a novel splicing factor. PLoS One **2,**
865 e471.

866 **Ananieva, E.A., Gillaspy, G.E., Ely, A., Burnette, R.N., and Erickson, F.L.** (2008).
867 Interaction of the WD40 domain of a myoinositol polyphosphate 5-phosphatase with
868 SnRK1 links inositol, sugar, and stress signaling. Plant Physiol **148,** 1868-1882.

869 **Anko, M.L., Muller-McNicoll, M., Brandl, H., Curk, T., Gorup, C., Henry, I., Ule, J., and**
870 **Neugebauer, K.M.** (2012). The RNA-binding landscapes of two SR proteins reveal
871 unique functions and binding to diverse RNA classes. Genome Biol **13,** R17.

872 **Ausin, I., Greenberg, M.V., Li, C.F., and Jacobsen, S.E.** (2012). The splicing factor SR45
873 affects the RNA-directed DNA methylation pathway in Arabidopsis. Epigenetics **7,** 29-
874 33.

Baena-Gonzalez, E., and Sheen, J. (2008). Convergent energy and stress signaling. Trends Plant Sci **13,** 474-482.

Baena-Gonzalez, E., Rolland, F., Thevelein, J.M., and Sheen, J. (2007). A central integrator of transcription networks in plant stress and energy signalling. Nature **448,** 938-942.

Baldwin, K.L., Dinh, E.M., Hart, B.M., and Masson, P.H. (2013). CACTIN is an essential nuclear protein in Arabidopsis and may be associated with the eukaryotic spliceosome. FEBS letters **587,** 873-879.

Barta, A., Kalyna, M., and Reddy, A.S. (2010). Implementing a rational and consistent nomenclature for serine/arginine-rich protein splicing factors (SR proteins) in plants. The Plant cell **22,** 2926-2929.

Bhalerao, R.P., Salchert, K., Bako, L., Okresz, L., Szabados, L., Muranaka, T., Machida, Y., Schell, J., and Koncz, C. (1999). Regulatory interaction of PRL1 WD protein with Arabidopsis SNF1-like protein kinases. Proc Natl Acad Sci U S A **96,** 5322-5327.

Carvalho, R.F., Carvalho, S.D., and Duque, P. (2010). The plant-specific SR45 protein negatively regulates glucose and ABA signaling during early seedling development in Arabidopsis. Plant Physiol **154,** 772-783.

Crozet, P., Margalha, L., Butowt, R., Fernandes, N., Elias, C.A., Orosa, B., Tomanov, K., Teige, M., Bachmair, A., Sadanandom, A., and Baena-Gonzalez, E. (2016). SUMOylation represses SnRK1 signaling in Arabidopsis. The Plant journal : for cell and molecular biology **85,** 120-133.

Dai, N., Schaffer, A., Petreikov, M., Shahak, Y., Giller, Y., Ratner, K., Levine, A., and Granot, D. (1999). Overexpression of Arabidopsis hexokinase in tomato plants inhibits growth, reduces photosynthesis, and induces rapid senescence. The Plant cell **11,** 1253-1266.

Day, I.S., Golovkin, M., Palusa, S.G., Link, A., Ali, G.S., Thomas, J., Richardson, D.N., and Reddy, A.S. (2012). Interactions of SR45, an SR-like protein, with spliceosomal

proteins and an intronic sequence: insights into regulated splicing. The Plant journal : for cell and molecular biology **71,** 936-947.

Feng, J., Li, J., Gao, Z., Lu, Y., Yu, J., Zheng, Q., Yan, S., Zhang, W., He, H., Ma, L., and Zhu, Z. (2015). SKIP Confers Osmotic Tolerance during Salt Stress by Controlling Alternative Gene Splicing in Arabidopsis. Molecular plant **8,** 1038-1052.

Filichkin, S.A., Cumbie, J.S., Dharmawardhana, P., Jaiswal, P., Chang, J.H., Palusa, S.G., Reddy, A.S., Megraw, M., and Mockler, T.C. (2015). Environmental stresses modulate abundance and timing of alternatively spliced circadian transcripts in Arabidopsis. Molecular plant **8,** 207-227.

Gabriel, B., Zur Hausen, A., Bouda, J., Boudova, L., Koprivova, M., Hirschfeld, M., Jager, M., and Stickeler, E. (2009). Significance of nuclear hTra2-beta1 expression in cervical cancer. Acta Obstet Gynecol Scand **88,** 216-221.

Gibson, S.I. (2005). Control of plant development and gene expression by sugar signaling. Curr Opin Plant Biol **8,** 93-102.

Golovkin, M., and Reddy, A.S. (1999). An SC35-like protein and a novel serine/arginine-rich protein interact with Arabidopsis U1-70K protein. The Journal of biological chemistry **274,** 36428-36438.

Jang, J.C., and Sheen, J. (1994). Sugar sensing in higher plants. The Plant cell **6,** 1665-1679.

Jang, J.C., Leon, P., Zhou, L., and Sheen, J. (1997). Hexokinase as a sugar sensor in higher plants. The Plant cell **9,** 5-19.

Jiang, Z., Tang, H., Havlioglu, N., Zhang, X., Stamm, S., Yan, R., and Wu, J.Y. (2003). Mutations in tau gene exon 10 associated with FTDP-17 alter the activity of an exonic splicing enhancer to interact with Tra2 beta. The Journal of biological chemistry **278,** 18997-19007.

Jossier, M., Bouly, J.P., Meimoun, P., Arjmand, A., Lessard, P., Hawley, S., Grahame Hardie, D., and Thomas, M. (2009). SnRK1 (SNF1-related kinase 1) has a central role

in sugar and ABA signalling in Arabidopsis thaliana. The Plant journal : for cell and molecular biology **59,** 316-328.

Kajita, K., Kuwano, Y., Kitamura, N., Satake, Y., Nishida, K., Kurokawa, K., Akaike, Y., Honda, M., Masuda, K., and Rokutan, K. (2013). Ets1 and heat shock factor 1 regulate transcription of the Transformer 2beta gene in human colon cancer cells. J Gastroenterol **48,** 1222-1233.

Kalyna, M., Lopato, S., and Barta, A. (2003). Ectopic expression of atRSZ33 reveals its function in splicing and causes pleiotropic changes in development. Mol Biol Cell **14,** 3565-3577.

Kim, J., and Chung, I.K. (2014). The splicing factor U2AF65 stabilizes TRF1 protein by inhibiting its ubiquitin-dependent proteolysis. Biochem Biophys Res Commun **443,** 1124-1130.

Kiryu-Seo, S., Matsuo, N., Wanaka, A., Ogawa, S., Tohyama, M., and Kiyama, H. (1998). A sequence-specific splicing activator, tra2beta, is up-regulated in response to nerve injury. Brain Res Mol Brain Res **62,** 220-223.

Koch, K.E. (1996). Carbohydrate-Modulated Gene Expression in Plants. Annu Rev Plant Physiol Plant Mol Biol **47,** 509-540.

Kohtz, J.D., Jamison, S.F., Will, C.L., Zuo, P., Luhrmann, R., Garcia-Blanco, M.A., and Manley, J.L. (1994). Protein-protein interactions and 5'-splice-site recognition in mammalian mRNA precursors. Nature **368,** 119-124.

Le Hir, H., Gatfield, D., Izaurralde, E., and Moore, M.J. (2001). The exon-exon junction complex provides a binding platform for factors involved in mRNA export and nonsense-mediated mRNA decay. EMBO J **20,** 4987-4997.

Lee, J.H., Terzaghi, W., Gusmaroli, G., Charron, J.B., Yoon, H.J., Chen, H., He, Y.J., Xiong, Y., and Deng, X.W. (2008). Characterization of Arabidopsis and rice DWD proteins and their roles as substrate receptors for CUL4-RING E3 ubiquitin ligases. The Plant cell **20,** 152-167.

Lee, K.W., Chen, P.W., Lu, C.A., Chen, S., Ho, T.H., and Yu, S.M. (2009). Coordinated responses to oxygen and sugar deficiency allow rice seedlings to tolerate flooding. Sci Signal **2,** ra61.

Li, X., Niu, T., and Manley, J.L. (2007). The RNA binding protein RNPS1 alleviates ASF/SF2 depletion-induced genomic instability. RNA **13,** 2108-2115.

Lin, S., and Fu, X.D. (2007). SR proteins and related factors in alternative splicing. Adv Exp Med Biol **623,** 107-122.

Lopato, S., Kalyna, M., Dorner, S., Kobayashi, R., Krainer, A.R., and Barta, A. (1999). atSRp30, one of two SF2/ASF-like proteins from Arabidopsis thaliana, regulates splicing of specific plant genes. Genes Dev **13,** 987-1001.

Lopez-Molina, L., Mongrand, S., and Chua, N.H. (2001). A postgermination developmental arrest checkpoint is mediated by abscisic acid and requires the ABI5 transcription factor in Arabidopsis. Proc Natl Acad Sci U S A **98,** 4782-4787.

Lykke-Andersen, J., Shu, M.D., and Steitz, J.A. (2001). Communication of the position of exon-exon junctions to the mRNA surveillance machinery by the protein RNPS1. Science **293,** 1836-1839.

Mair, A., Pedrotti, L., Wurzinger, B., Anrather, D., Simeunovic, A., Weiste, C., Valerio, C., Dietrich, K., Kirchler, T., Nagele, T., Vicente Carbajosa, J., Hanson, J., Baena-Gonzalez, E., Chaban, C., Weckwerth, W., Droge-Laser, W., and Teige, M. (2015). SnRK1-triggered switch of bZIP63 dimerization mediates the low-energy response in plants. eLife **4**.

Marquez, Y., Hopfler, M., Ayatollahi, Z., Barta, A., and Kalyna, M. (2015). Unmasking alternative splicing inside protein-coding exons defines exitrons and their role in proteome plasticity. Genome Res **25,** 995-1007.

Mayeda, A., Badolato, J., Kobayashi, R., Zhang, M.Q., Gardiner, E.M., and Krainer, A.R. (1999). Purification and characterization of human RNPS1: a general activator of pre-mRNA splicing. EMBO J **18,** 4560-4570.

McKibbin, R.S., Muttucumaru, N., Paul, M.J., Powers, S.J., Burrell, M.M., Coates, S., Purcell, P.C., Tiessen, A., Geigenberger, P., and Halford, N.G. (2006). Production of high-starch, low-glucose potatoes through over-expression of the metabolic regulator SnRK1. Plant Biotechnol J **4,** 409-418.

Moore, B., Zhou, L., Rolland, F., Hall, Q., Cheng, W.H., Liu, Y.X., Hwang, I., Jones, T., and Sheen, J. (2003). Role of the Arabidopsis glucose sensor HXK1 in nutrient, light, and hormonal signaling. Science **300,** 332-336.

Muller, P.Y., Janovjak, H., Miserez, A.R., and Dobbie, Z. (2002). Processing of gene expression data generated by quantitative real-time RT-PCR. BioTechniques **32,** 1372-1374, 1376, 1378-1379.

Palusa, S.G., Ali, G.S., and Reddy, A.S. (2007). Alternative splicing of pre-mRNAs of Arabidopsis serine/arginine-rich proteins: regulation by hormones and stresses. The Plant journal : for cell and molecular biology **49,** 1091-1107.

Pelisch, F., Gerez, J., Druker, J., Schor, I.E., Munoz, M.J., Risso, G., Petrillo, E., Westman, B.J., Lamond, A.I., Arzt, E., and Srebrow, A. (2010). The serine/arginine-rich protein SF2/ASF regulates protein sumoylation. Proc Natl Acad Sci U S A **107,** 16119-16124.

Pendle, A.F., Clark, G.P., Boon, R., Lewandowska, D., Lam, Y.W., Andersen, J., Mann, M., Lamond, A.I., Brown, J.W., and Shaw, P.J. (2005). Proteomic analysis of the Arabidopsis nucleolus suggests novel nucleolar functions. Mol Biol Cell **16,** 260-269.

Price, J., Laxmi, A., St Martin, S.K., and Jang, J.C. (2004). Global transcription profiling reveals multiple sugar signal transduction mechanisms in Arabidopsis. The Plant cell **16,** 2128-2150.

Purcell, P.C., Smith, A.M., and Halford, N.G. (1998). Antisense expression of a sucrose non-fermenting-1-related protein kinase sequence in potato results in decreased expression of sucrose synthase in tubers and loss of sucrose-inducibility of sucrose synthase transcripts in leaves. Plant Journal **14,** 195-202.

Radchuk, R., Radchuk, V., Weschke, W., Borisjuk, L., and Weber, H. (2006). Repressing the expression of the SUCROSE NONFERMENTING-1-RELATED

PROTEIN KINASE gene in pea embryo causes pleiotropic defects of maturation similar to an abscisic acid-insensitive phenotype. Plant Physiol **140,** 263-278.

Radchuk, R., Emery, R.J., Weier, D., Vigeolas, H., Geigenberger, P., Lunn, J.E., Feil, R., Weschke, W., and Weber, H. (2010). Sucrose non-fermenting kinase 1 (SnRK1) coordinates metabolic and hormonal signals during pea cotyledon growth and differentiation. The Plant journal : for cell and molecular biology **61,** 324-338.

Remy, E., Cabrito, T.R., Batista, R.A., Hussein, M.A., Teixeira, M.C., Athanasiadis, A., Sa-Correia, I., and Duque, P. (2014). Intron retention in the 5'UTR of the novel ZIF2 transporter enhances translation to promote zinc tolerance in arabidopsis. PLoS genetics **10,** e1004375.

Rodrigues, A., Adamo, M., Crozet, P., Margalha, L., Confraria, A., Martinho, C., Elias, A., Rabissi, A., Lumbreras, V., Gonzalez-Guzman, M., Antoni, R., Rodriguez, P.L., and Baena-Gonzalez, E. (2013). ABI1 and PP2CA phosphatases are negative regulators of Snf1-related protein kinase1 signaling in Arabidopsis. The Plant cell **25,** 3871-3884.

Rolland, F., Baena-Gonzalez, E., and Sheen, J. (2006). Sugar sensing and signaling in plants: conserved and novel mechanisms. Annu Rev Plant Biol **57,** 675-709.

Ruan, Y.L. (2014). Sucrose metabolism: gateway to diverse carbon use and sugar signaling. Annu Rev Plant Biol **65,** 33-67.

Sakashita, E., Tatsumi, S., Werner, D., Endo, H., and Mayeda, A. (2004). Human RNPS1 and its associated factors: a versatile alternative pre-mRNA splicing regulator in vivo. Molecular and cellular biology **24,** 1174-1187.

Sanford, J.R., Wang, X., Mort, M., Vanduyn, N., Cooper, D.N., Mooney, S.D., Edenberg, H.J., and Liu, Y. (2009). Splicing factor SFRS1 recognizes a functionally diverse landscape of RNA transcripts. Genome Res **19,** 381-394.

Simpson, C.G., Fuller, J., Maronova, M., Kalyna, M., Davidson, D., McNicol, J., Barta, A., and Brown, J.W. (2008). Monitoring changes in alternative precursor messenger RNA splicing in multiple gene transcripts. The Plant journal : for cell and molecular biology **53,** 1035-1048.

Stankovic, N., Schloesser, M., Joris, M., Sauvage, E., Hanikenne, M., and Motte, P. (2016). Dynamic Distribution and Interaction of the Arabidopsis SRSF1 Subfamily Splicing Factors. Plant Physiol **170,** 1000-1013.

Thomas, J., Palusa, S.G., Prasad, K.V., Ali, G.S., Surabhi, G.K., Ben-Hur, A., Abdel-Ghany, S.E., and Reddy, A.S. (2012). Identification of an intronic splicing regulatory element involved in auto-regulation of alternative splicing of SCL33 pre-mRNA. The Plant journal : for cell and molecular biology.

Tiessen, A., Prescha, K., Branscheid, A., Palacios, N., McKibbin, R., Halford, N.G., and Geigenberger, P. (2003). Evidence that SNF1-related kinase and hexokinase are involved in separate sugar-signalling pathways modulating post-translational redox activation of ADP-glucose pyrophosphorylase in potato tubers. The Plant journal : for cell and molecular biology **35,** 490-500.

Tsai, A.Y., and Gazzarrini, S. (2012). Overlapping and distinct roles of AKIN10 and FUSCA3 in ABA and sugar signaling during seed germination. Plant Signal Behav **7,** 1238-1242.

Wahl, M.C., Will, C.L., and Luhrmann, R. (2009). The spliceosome: design principles of a dynamic RNP machine. Cell **136,** 701-718.

Wang, X., Wu, F., Xie, Q., Wang, H., Wang, Y., Yue, Y., Gahura, O., Ma, S., Liu, L., Cao, Y., Jiao, Y., Puta, F., McClung, C.R., Xu, X., and Ma, L. (2012). SKIP is a component of the spliceosome linking alternative splicing and the circadian clock in Arabidopsis. The Plant cell **24,** 3278-3295.

Watermann, D.O., Tang, Y., Zur Hausen, A., Jager, M., Stamm, S., and Stickeler, E. (2006). Splicing factor Tra2-beta1 is specifically induced in breast cancer and regulates alternative splicing of the CD44 gene. Cancer Res **66,** 4774-4780.

Wu, S., Romfo, C.M., Nilsen, T.W., and Green, M.R. (1999). Functional recognition of the 3' splice site AG by the splicing factor U2AF35. Nature **402,** 832-835.

Xiao, W., Sheen, J., and Jang, J.C. (2000). The role of hexokinase in plant sugar signal transduction and growth and development. Plant molecular biology **44,** 451-461.

Xing, D., Wang, Y., Hamilton, M., Ben-Hur, A., and Reddy, A.S. (2015). Transcriptome-Wide Identification of RNA Targets of Arabidopsis SERINE/ARGININE-RICH45 Uncovers the Unexpected Roles of This RNA Binding Protein in RNA Processing. The Plant cell **27,** 3294-3308.

Zhang, X.N., and Mount, S.M. (2009). Two alternatively spliced isoforms of the Arabidopsis SR45 protein have distinct roles during normal plant development. Plant Physiol **150,** 1450-1458.

Zhang, X.N., Mo, C., Garrett, W.M., and Cooper, B. (2014). Phosphothreonine 218 is required for the function of SR45.1 in regulating flower petal development in Arabidopsis. Plant Signal Behav **9**.

Zhuang, Y., and Weiner, A.M. (1986). A compensatory base change in U1 snRNA suppresses a 5' splice site mutation. Cell **46,** 827-835.

Figure 1

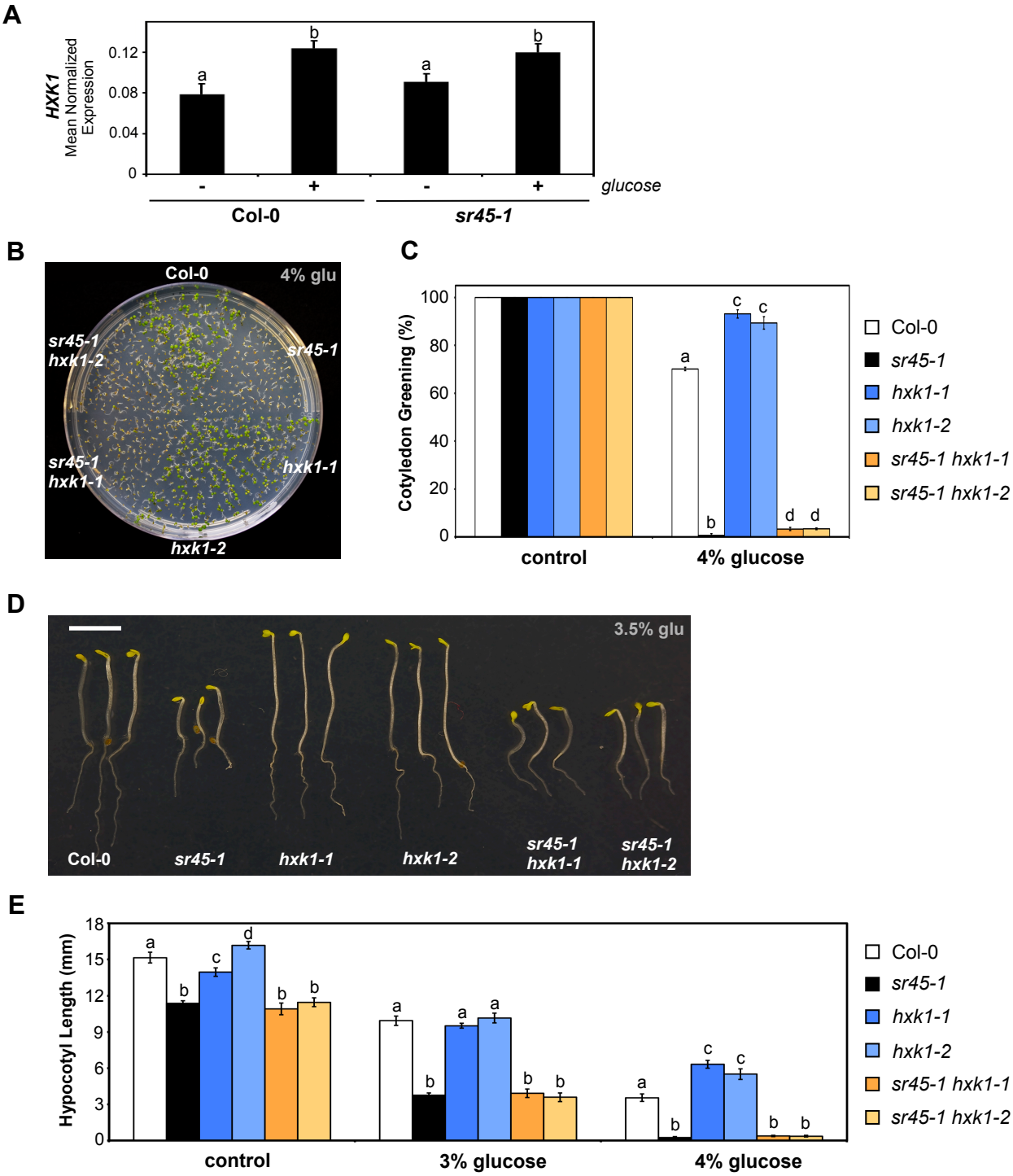

Figure 1. HXK1 Dependency of the *sr45-1* Glucose Phenotypes.

(A) RT-qPCR analysis of *HXK1* transcript levels in wild-type (Col-0) and *sr45-1* mutant leaves treated or not with 1.5% glucose, using *ACT2* as a reference gene. Results are from two independent experiments and values represent means ± SE (n = 4). Different letters indicate statistically significant differences ($P < 0.05$; Student's t-test).

(B) Representative image of seedlings of the wild type (Col-0), the *sr45-1*, *hxk1-1* and *hxk1-2* single mutants and the *sr45-1 hxk1-1* and *sr45-1 hxk1-2* double mutants, grown in the presence of 4% glucose for 7 d.

(C) Cotyledon greening rates, scored 7 d after stratification, of seedlings of the wild type (Col-0), the *sr45-1*, *hxk1-1* and *hxk1-2* single mutants and the *sr45-1 hxk1-1* and *sr45-1 hxk1-2* double mutants, grown under control conditions or in the presence of 4% glucose (means ± SE, n = 3). Different letters indicate statistically significant differences between genotypes under each condition ($P < 0.05$; Student's t-test).

(D) Representative image of seedlings of the wild type (Col-0), the *sr45-1*, *hxk1-1* and *hxk1-2* single mutants and the *sr45-1 hxk1-1* and *sr45-1 hxk1-2* double mutants, grown in the dark in the presence of 3.5% glucose for 7 d. Bar = 8 mm.

(E) Hypocotyl length, measured 7 d after stratification, of seedlings of the wild type (Col-0), the *sr45-1*, *hxk1-1* and *hxk1-2* single mutants and the *sr45-1 hxk1-1* and *sr45-1 hxk1-2* double mutants, grown in the dark under control conditions or in the presence of 3% or 4% glucose (means ± SE, n = 30-60). Different letters indicate statistically significant differences between genotypes under each condition ($P < 0.05$; Student's t-test).

Figure 2

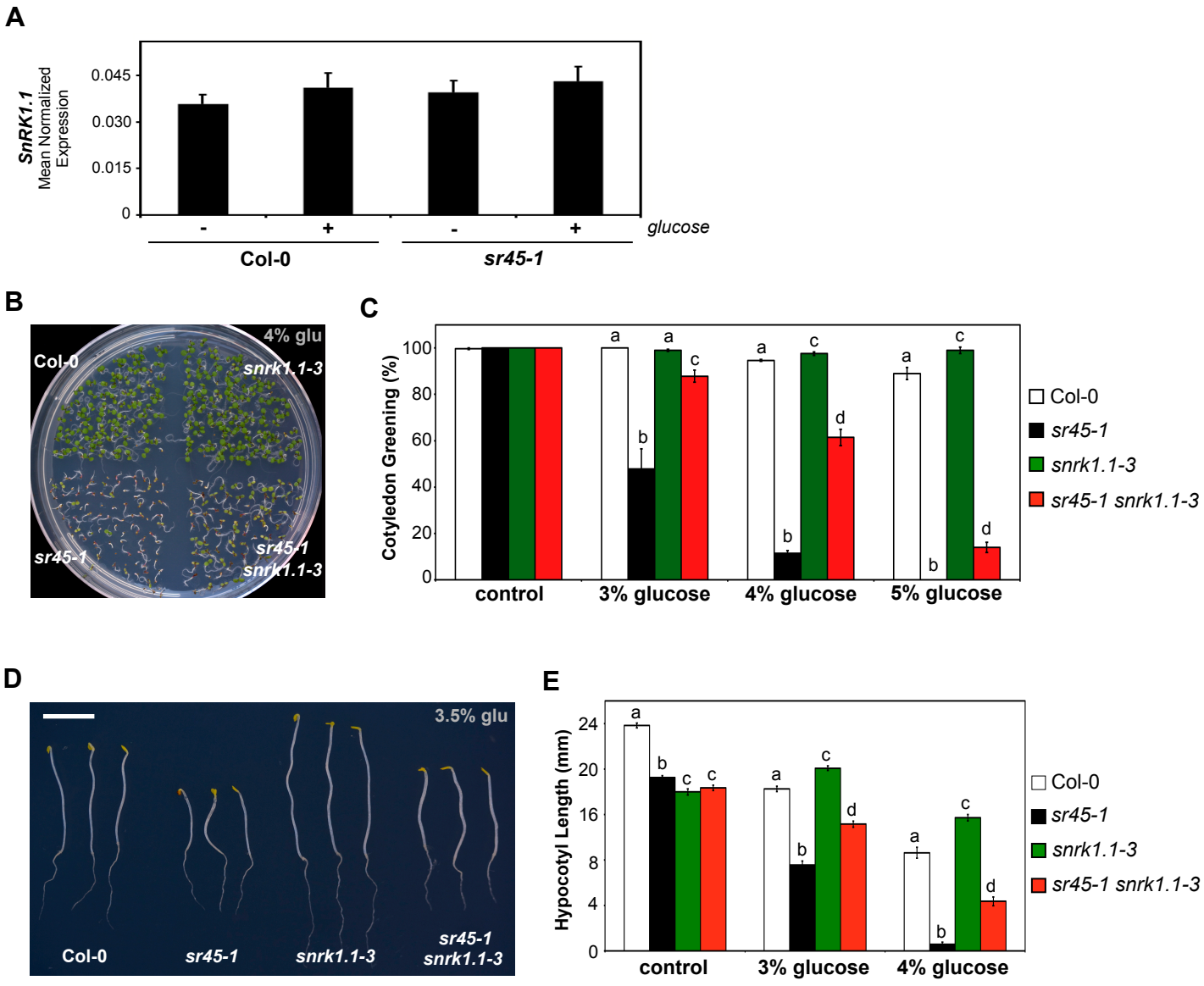

Figure 2. SnRK1.1 Dependency of the *sr45-1* Glucose Phenotypes.

(A) RT-qPCR analysis of *SnRK1.1* transcript levels in wild-type (Col-0) and *sr45-1* mutant leaves incubated in the absence or presence of 1.5% glucose, using *ACT2* as a reference gene. Results are from two independent experiments and values represent means ± SE (*n* = 4). No statistically significant differences between samples were detected (P > 0.05; Student's *t*-test).
(B) Representative image of seedlings of the wild type (Col-0), the *sr45-1* and *snrk1.1-3* single mutants and the *sr45-1 snrk1.1-3* double mutant grown in the presence of 4% glucose for 7 d.
(C) Cotyledon greening rates, scored 7 d after stratification, of seedlings of the wild type (Col-0), the *sr45-1* and *snrk1.1-3* single mutants and the *sr45-1 snrk1.1-3* double mutant, grown under control conditions or in the presence of 3%, 4% or 5% glucose (means ± SE, *n* = 3). Different letters indicate statistically significant differences between genotypes under each condition (P < 0.05; Student's *t*-test).
(D) Representative image of seedlings of the wild type (Col-0), the *sr45-1* and *snrk1.1-3* single mutants and the *sr45-1 snrk1.1-3* double mutant, grown in the dark in the presence of 3.5% glucose for 7 d. Bar = 10 mm.
(E) Hypocotyl length, measured 7 d after stratification, of seedlings of the wild type (Col-0), the *sr45-1* and *snrk1.1-3* single mutants and the *sr45-1 snrk1.1-3* double mutant, grown in the dark under control conditions or in the presence of 3% or 4% glucose (means ± SE, *n* = 40-60). Different letters indicate statistically significant differences between genotypes under each condition (P < 0.05; Student's *t*-test).

Figure 3

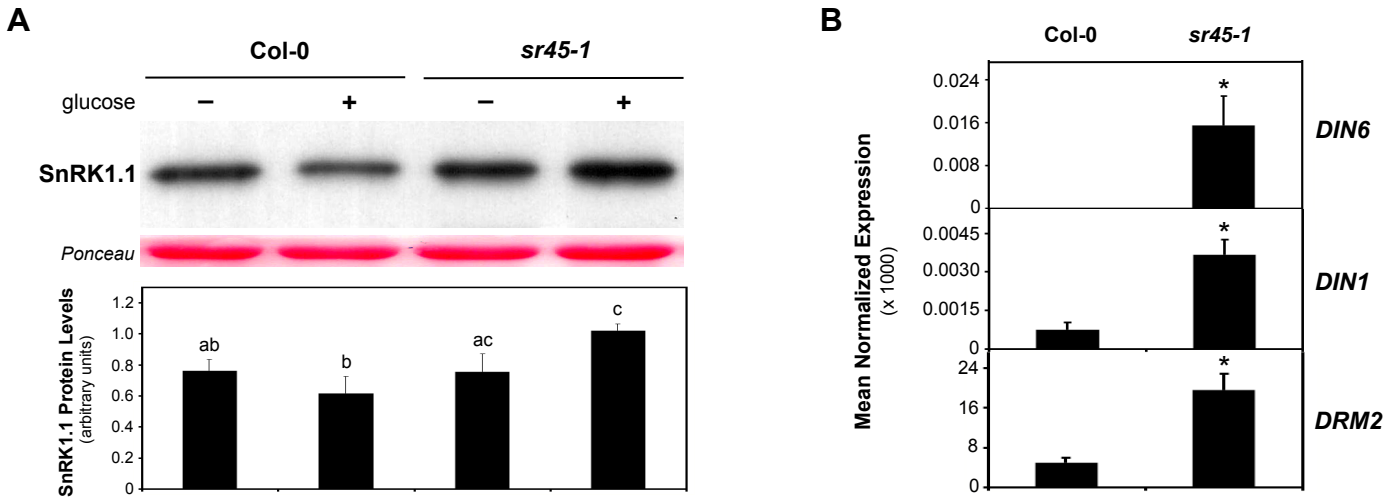

Figure 3. SR45 Modulation of SnRK1.1 Protein Levels and SnRK1.1-Activated Genes.

(A) Protein gel blot analysis of SnRK1.1 levels in wild-type (Col-0) and *sr45-1* mutant leaves incubated in the absence or presence of 1.5% glucose. Bands were quantified and relative protein levels determined using the Ponceau loading control as a reference. The blot image is representative of four independent experiments, and the bar graph shows means ± SE of SnRK1.1 protein levels in all assays (n = 4). Different letters indicate statistically significant differences ($P < 0.05$; Student's t-test).

(B) RT-qPCR analysis of the transcript levels of SnRK1.1 marker genes *DIN6, DIN1* and *DRM2* in wild-type (Col-0) and *sr45-1* mutant leaves incubated in the presence of 1.5% glucose, using *EF1A* as a reference gene. Results are from two independent experiments and values represent means ± SE (n = 4). Asterisks indicate statistically significant differences from the wild type ($P < 0.05$; Student's t-test).

Figure 5

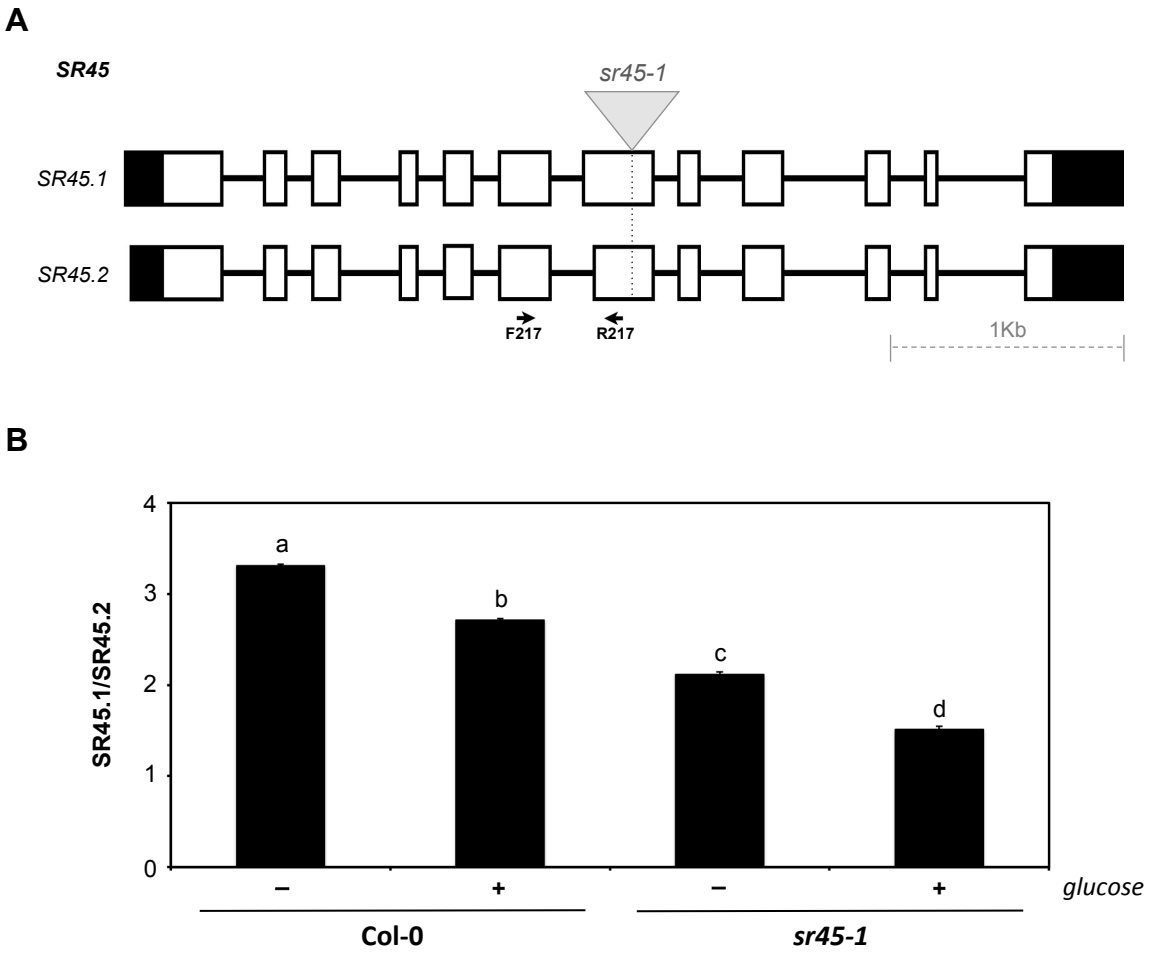

Figure 5. Effect of *sr45-1* Mutation on Alternative Splicing of the *SR45* Pre-mRNA.

(A) Schematic diagram of two splice variants (*SR45.1* and *SR45.2*) produced by the *Arabidopsis SR45* gene. Boxes represent exons with UTRs in black, lines represent introns and the inverted triangle indicates the position of the T-DNA insertion in the *sr45-1* mutant allele. The arrows indicate the location of the primer pair used in the RT-PCR panel, where the sizes of the PCR products obtained for the *SR45.1* and *SR45.2* splice variants were 177 and 156 bp, respectively.
(B) Histogram showing the ratio between the abundance of the *SR45.1* and *SR45.2* splice variants in wild-type (Col-0) and *sr45-1* mutant seedlings grown under control conditions or in the presence of 3% glucose (means ± SE, *n* = 4). Different letters indicate statistically significant differences ($P < 0.05$, Student's *t*-test).

Figure 6

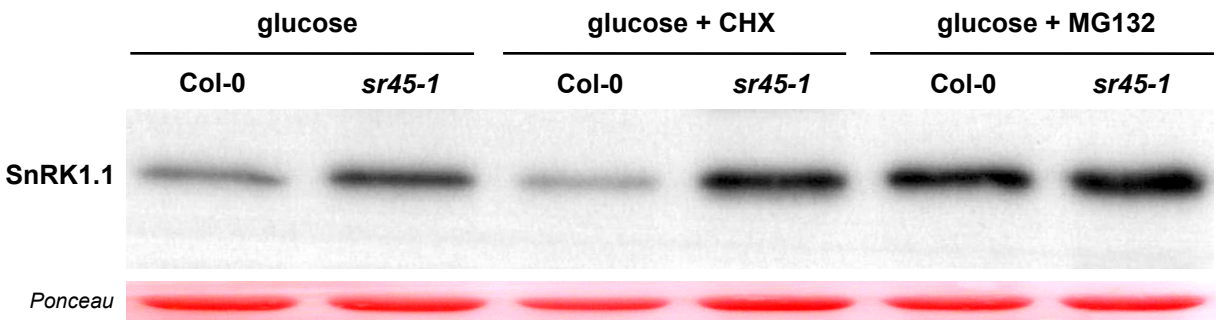

Figure 6. Effect of SR45 on SnRK1.1 Proteasomal Degradation.

Protein gel blot analysis of SnRK1.1 levels in leaves treated with 1.5% glucose in the absence or presence of 100 µM of the protein synthesis inhibitor cycloheximide (CHX) or of 50 µM of the proteasome inhibitor MG132 (Ponceau-stained membrane is shown as a loading control).

Figure 7

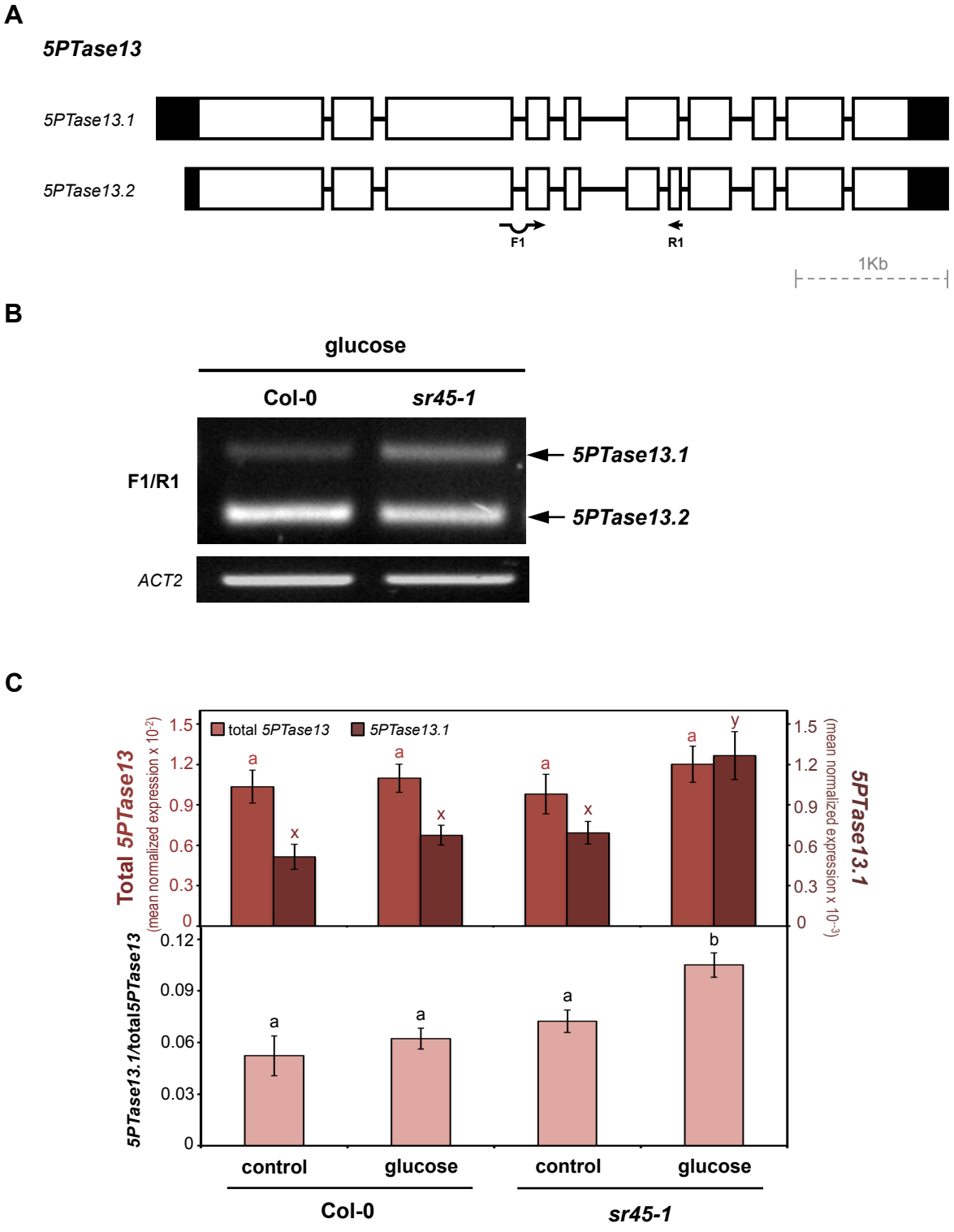

Figure 7. SR45 Regulation of Alternative Splicing of the *5PTase13* Pre-mRNA.

(A) Schematic diagram of two splice variants (*5PTase13.1* and *5PTase13.2*) produced by the *Arabidopsis 5PTase13* gene. Boxes represent exons with UTRs in black, lines represent introns, and arrows indicate the location of the *5PTase13* F1 and R1 primers.

(B) RT-PCR analysis of *5PTase13* transcript levels in wild-type (Col-0) and *sr45-1* mutant leaves incubated in the presence of 1.5% glucose. The location of the F1 and R1 primers used is shown in **(A).** Expression of the *ACT2* gene is shown as a loading control.

(C) RT-qPCR analysis of total *5PTase13* expression as well as *5PTase13.1* transcript levels (different Y-axis scales) in wild-type (Col-0) and *sr45*-1 mutant leaves incubated in the absence or presence of 1.5% glucose, using *EF1A* as a reference gene (upper panel). The expression ratio between *5PTase13.1* and total *5PTase13* is also shown (lower panel). Results are from two independent experiments and values represent means ± SE (*n* = 4). Different letters indicate statistically significant differences ($P < 0.05$; Student's *t*-test).

Figure 8

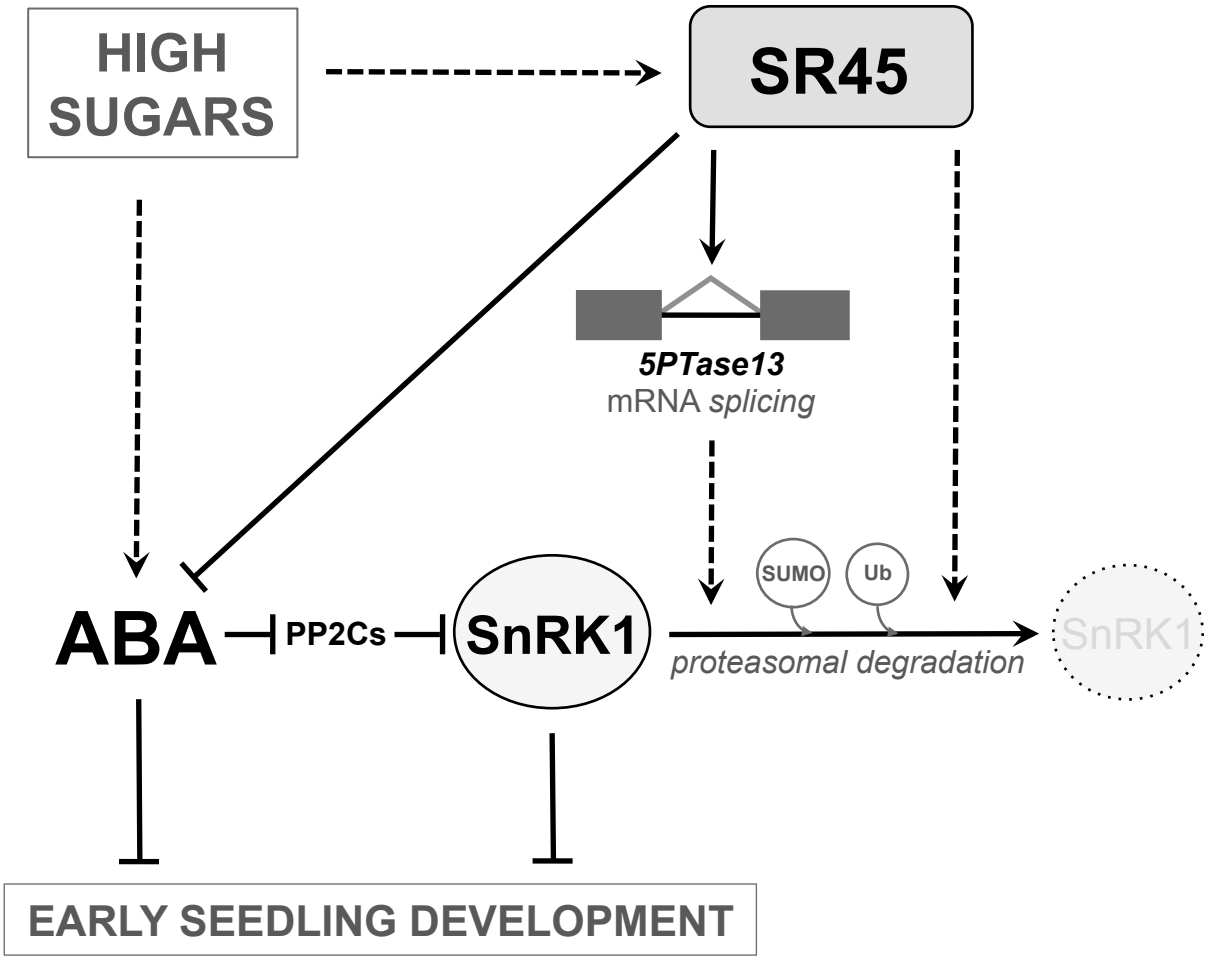

Figure 8. Model of SR45-Mediated Sugar Signaling During Early Seedling Development.

High sugars lead to an ABA-mediated early growth arrest in *Arabidopsis*. SR45 negatively regulates sugar signaling by repressing glucose-induced ABA accumulation (Carvalho et al., 2010). One component contributing to the regulation of sugar signaling by SR45 is the SnRK1 protein kinase, which is activated by ABA in a PP2C-dependent manner (Rodrigues et al., 2013) and whose overexpression in young *Arabidopsis* seedlings causes glucose and ABA hypersensitivity (Jossier et al., 2009; Tsai and Gazzarrini, 2012). SnRK1 activity is also regulated via SUMOylation/ubiquitination and subsequent degradation by the 26S proteasome (Lee at al., 2008; Crozet et al., 2016). The SR45 SR-like protein regulates SnRK1 protein levels in response to sugars by modulating alternative splicing of the *5PTase13* pre-mRNA — encoding a modulator of SnRK1 proteasomal degradation (Ananieva et al., 2008) — where excision of intron 6 promotes destabilization of the SnRK1 protein. Alternatively, SR45 could play a direct role in SnRK1 degradation via a non-splicing function.

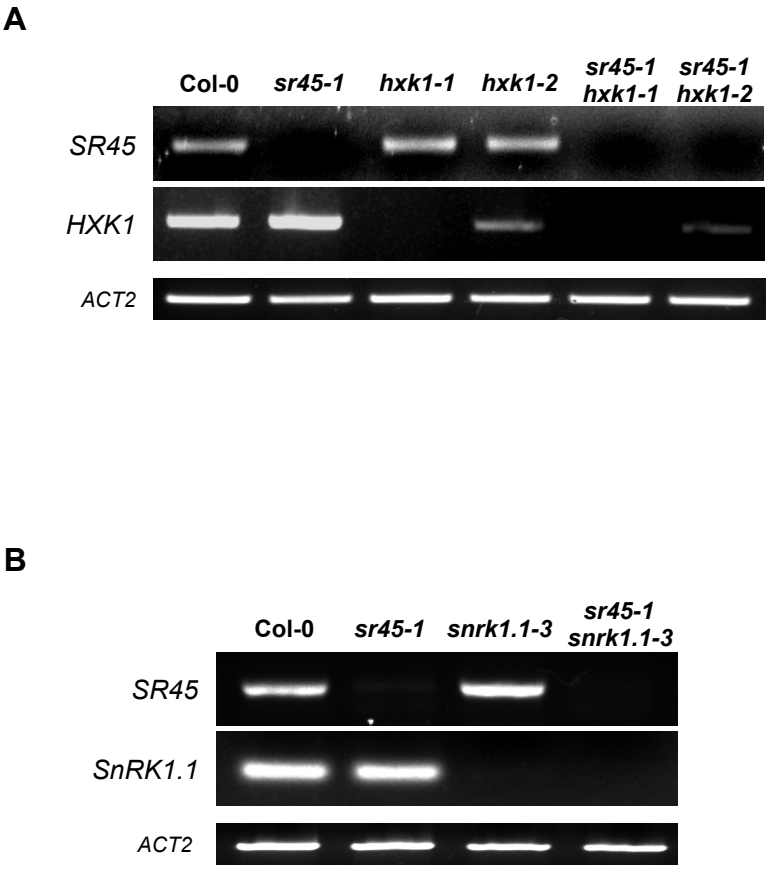

Supplemental Figure 1. mRNA Analysis of the *SR45, HXK1* and *SnRK1.1* Loss-of-Function Single and Double Mutants Used in This Study.

(A) RT-PCR analysis of *SR45* and *HXK1* transcript levels in seedlings of the wild type (Col-0), the *sr45-1*, *hxk1-1* and *hxk1-2* single mutants and the *sr45-1 hxk1-1* and *sr45-1 hxk1-2* double mutants.
(B) RT-PCR analysis of *SR45* and *SnRK1.1* transcript levels in seedlings of the wild-type (Col-0), the *sr45-1* and *snrk1.1-3* single mutants and the *sr45-1 snrk1.1-3* double mutant.
Expression of the *ACT2* gene is shown as a loading control. Results are representative of three independent experiments.

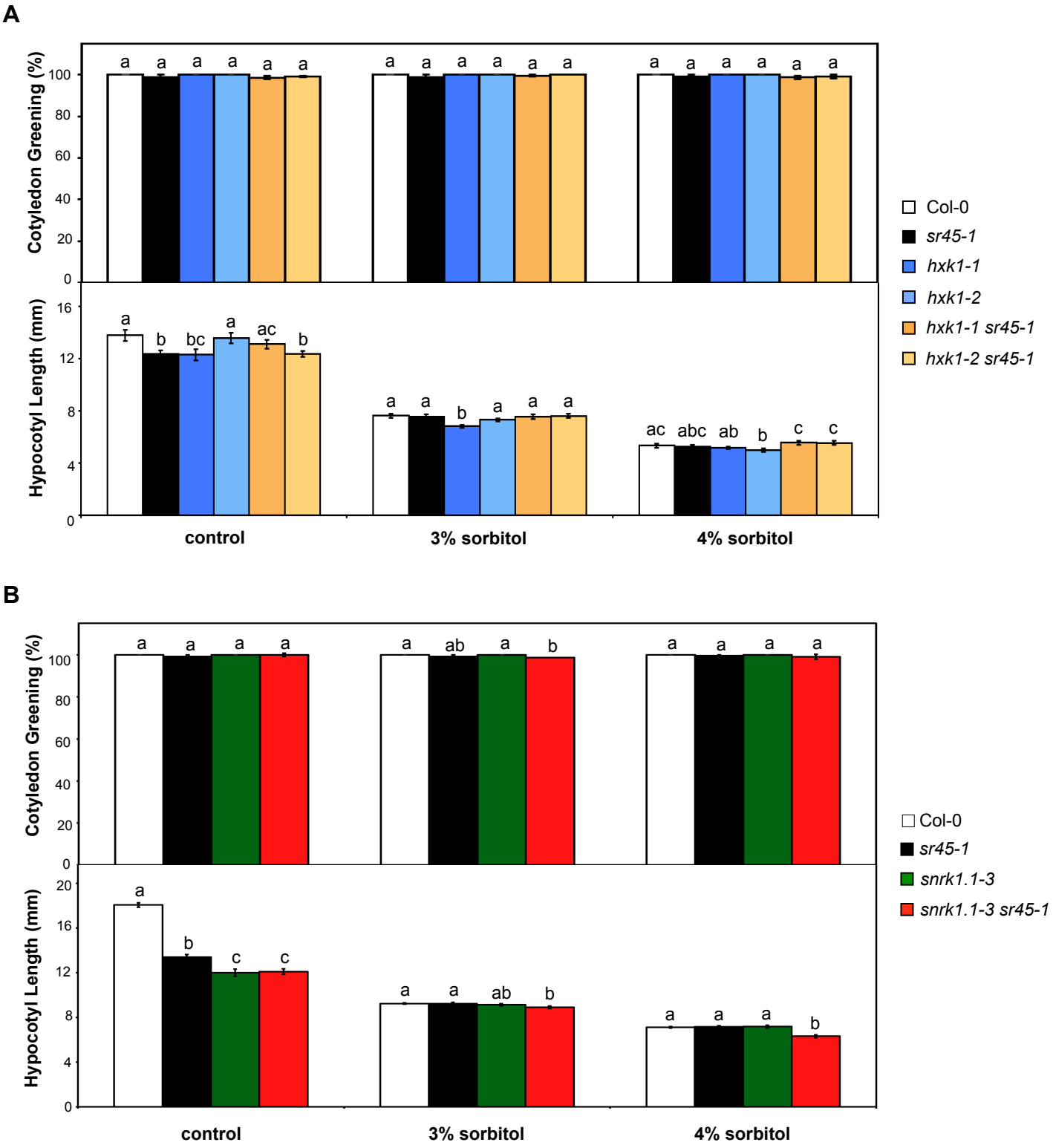

Supplemental Figure 2. Effect of Sorbitol on Cotyledon Greening and Hypocotyl Elongation.

(A) Cotyledon greening rates and hypocotyl length, scored 7 d after stratification, of seedlings of the wild type (Col-0), the *sr45-1*, *hxk1-1* and *hxk1-2* single mutants and the *hxk1-1 sr45-1* and *hxk1-2 sr45-1* double mutants, grown in the light (means ± SE, *n* = 3) or dark (means ± SE, *n* = 30-60), respectively, under control conditions or in the presence of 3% or 4% sorbitol.

(B) Cotyledon greening rates and hypocotyl length, scored 7 d after stratification, of seedlings of the wild type (Col-0), the *sr45-1* and *snrk1.1-3* single mutants and the *snrk1.1-3 sr45-1* double mutant, grown in the light (means ± SE, *n* = 3) or dark (means ± SE, *n* = 30-60), respectively, under control conditions or in the presence of 3% or 4% sorbitol.

Different letters indicate statistically significant differences between genotypes under each condition ($P < 0.05$; Student's *t*-test).

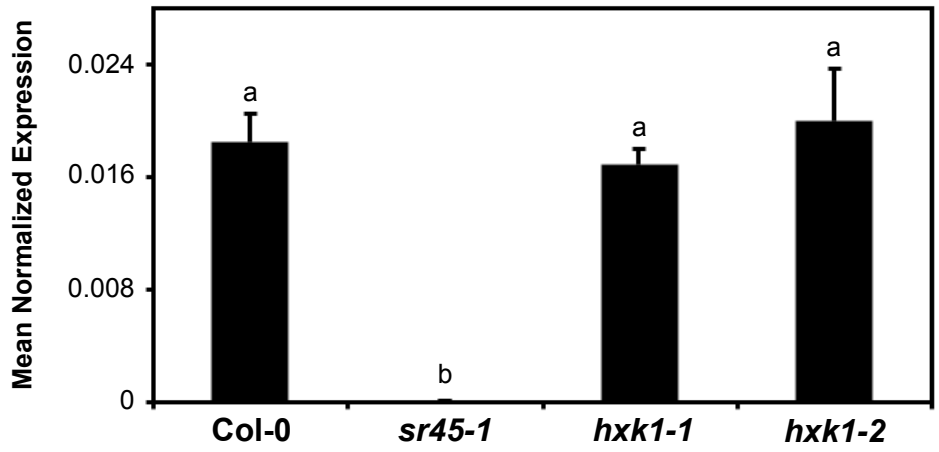

Supplemental Figure 3. *SR45* Expression Levels in the *hxk1* Loss-of-Function Mutants.

RT-qPCR analysis of *SR45* transcript levels in wild-type (Col-0) and *sr45-1, hxk1-1* and *hxk1-2* mutant seedlings grown in control conditions, using *ACT2* as a reference gene. Results are from two independent experiments and values represent means ± SE (*n* = 4). Different letters indicate statistically significant differences (P < 0.05; Student's *t*-test).

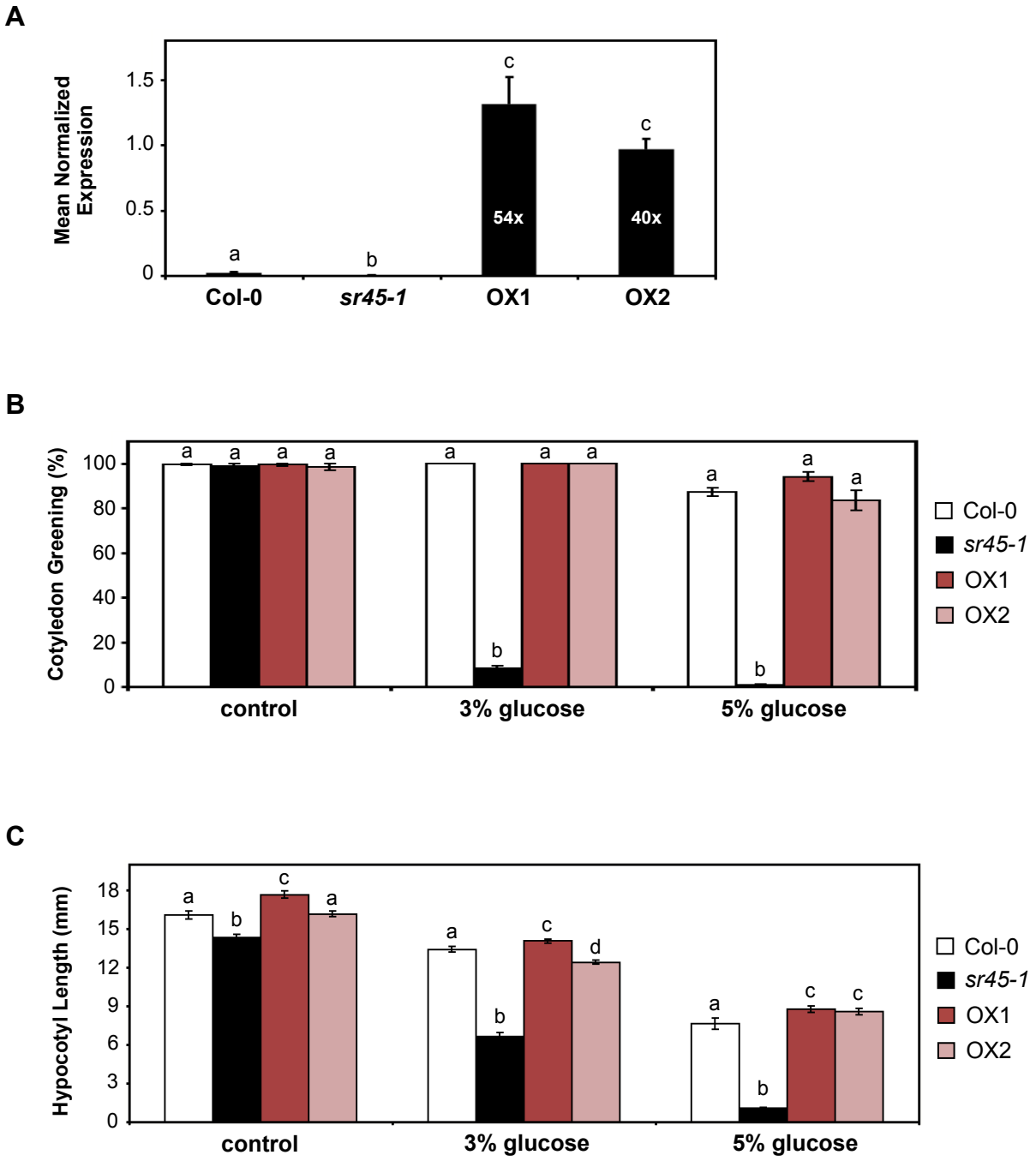

Supplemental Figure 4. Phenotypic Analysis of *SR45* Overexpressor Lines.

(A) RT-qPCR analysis of *SR45.1* transcript levels in seedlings of the wild-type (Col-0), the *sr45-1* mutant and two independent *SR45.1*-overexpressing lines, OX1 and OX2, grown under control conditions, using *ACT2* as a reference gene. Results are from two independent experiments and values represent means ± SE (*n* = 4). The magnitude of overexpression of the *SR45* transcript in the two transgenic lines relative to the wild type is indicated in white on the corresponding bars.

(B) Cotyledon greening rates, scored 7 d after stratification, of seedlings of the wild type (Col-0), the *sr45-1* mutant and two independent *SR45.1*-overexpressing lines, OX1 and OX2, grown under control conditions or in the presence of 3% or 5% glucose (means ± SE, *n* = 3).

(C) Hypocotyl length, measured 7 d after stratification, of seedlings of the wild type (Col-0), the *sr45-1* mutant and two independent *SR45.1*-overexpressing lines, OX1 and OX2, grown in the dark under control conditions or in the presence of 3% or 5% glucose (means ± SE, *n* = 30-60).

Different letters indicate statistically significant differences between genotypes under each condition ($P < 0.05$; Student's *t*-test).

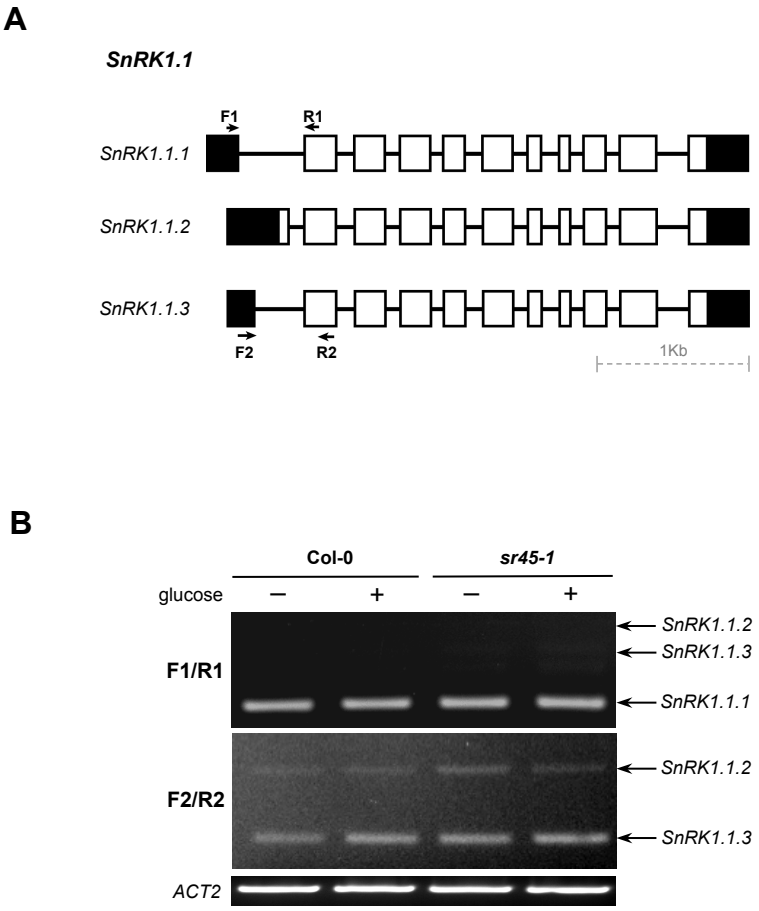

Supplemental Figure 5. Splicing Pattern of the *SnRK1.1* Gene.

(A) Schematic diagram of three splice variants produced by the *Arabidopsis SnRK1.1* gene. Boxes represent exons with UTRs in black and lines represent introns. The arrows indicate the location of the *SnRK1.1* F1, R1, F2 and R2 primers.
(B) RT-PCR analysis of *SnRK1.1* transcript levels in wild-type (Col-0) and *sr45-1* mutant leaves incubated in the absence or presence of 1.5% glucose. The location of the F1, R1, F2 and R2 primers used is shown in **(A)**. Expression of the *ACT2* gene is shown as a loading control. Results are representative of three independent experiments.

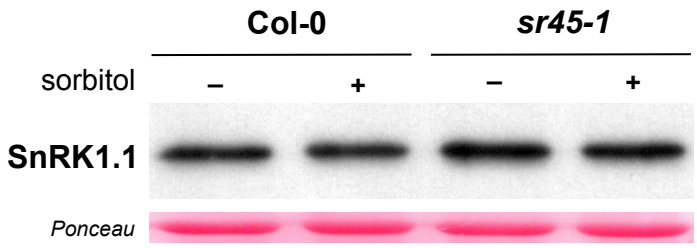

Supplemental Figure 6. Effect of Sorbitol on *sr45-1* SnRK1.1 Protein Levels.

SnRK1.1 protein levels in wild-type (Col-0) and *sr45-1* mutant leaves incubated for 6 h in the absence or presence of 1.5% sorbitol (Ponceau-stained membrane is shown as a loading control).

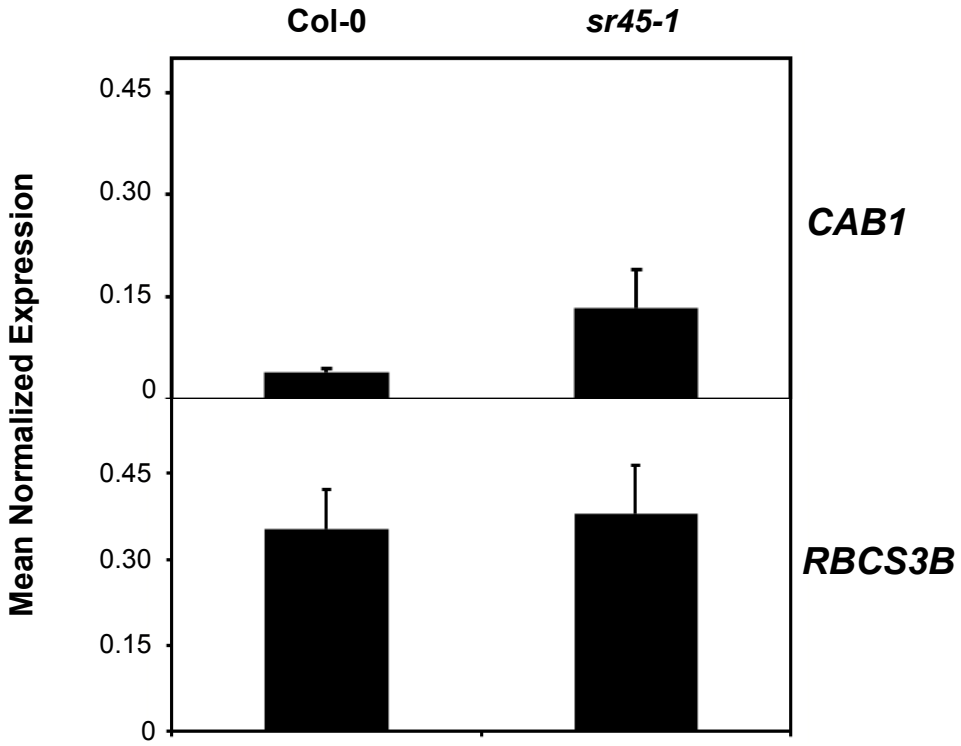

Supplemental Figure 7. Effect of *sr45-1* Mutation on Expression of the Photosynthesis-Related *CAB1* and *RBCS3B* Genes.

RT-qPCR analysis of the transcript levels of the *CAB1* and *RBCS3B* genes in wild-type (Col-0) and *sr45-1* mutant leaves incubated in the presence of 1.5% glucose, using *EF1A* as a reference gene. Results are from two independent experiments and values represent means ± SE (*n* = 4). For either gene, no statistically significant differences between genotypes were detected (P > 0.05; Student's *t*-test).

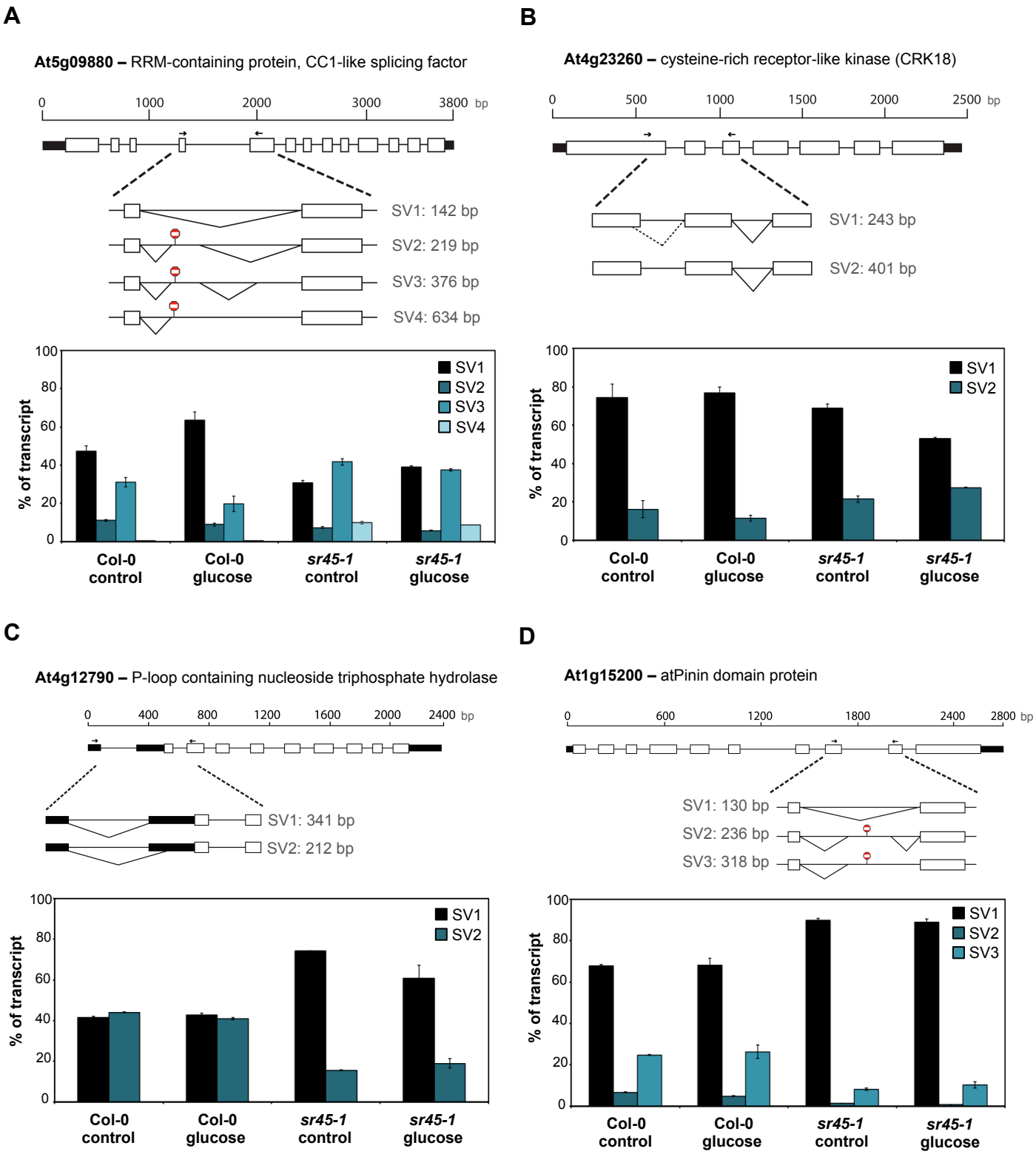

Supplemental Figure 8. Genes Showing Substantial Alternative Splicing Changes in the *sr45-1* Mutant.

The gene structure and the structure of the transcript isoforms around the alternative splicing event, as well as histograms showing the proportion of each transcript (means ± SE, *n* = 3) in wild-type (Col-0) and mutant (*sr45-1*) seedlings grown under control conditions or in the presence of 3% glucose, are shown for the At5g09880 **(A)**, At4g23260 **(B)**, At4g12790 **(C)** and At1g15200 **(D)** genes. In the schematic diagrams, boxes represent exons with UTRs in black, lines represent introns, diagonal lines represent the splicing events (dashed lines represent events not yet confirmed by sequencing) and stop signs represent premature termination codons (PTCs). The sizes of the PCR products from each splice isoform are indicated.

Supplemental Table 1. Sequences of the Primers Used

RT-qPCR Analyses

Gene ID	Primer Name	Primer Sequence (5' to 3')	Description
At4g29130	HXK1 F1	AAAGTTGTGATCAGTCTCTGC	*HXK1*-specific (Figure 1A)
	HXK1 R1	ATAACCGATTTCTGCACCTCC	
At3g01090	SnRK1.1 F1	ATGAAGTGCAGATGGGTTCC	*SnRK1.1*-specific (Figure 2A)
	SnRK1.1 R1	ACATTGGGCGACTTAACAGC	
At2g33830	DRM2 F1	CTTCGACAAGCCTTCTCACC	*DRM2*-specific (Figure 3B)
	DRM2 R1	TCGTCGCTGTATAGCCAATC	
At4g35770	DIN1 F1	CAGAGTCGGATCAGGAATGG	*DIN1*-specific (Figure 3B)
	DIN1 R1	ATTTGACCGCTCTCACAACC	
At3g47340	DIN6 F1	AAGAGGTGGCGGAATATTTGG	*DIN6*-specific (Figure 3B)
	DIN6 R1	TGTGCTCGCTCTGATAGTCG	
At1g05630	5PTase13 F2	TGGCTGCTTTATTCTTCTGG	*5PTase13*-specific, amplification of *5PTase13.1* (Figure 7C)
	5PTase13 R2	GTGCTTGGAATAGTGTTACTC	
	5PTase13 F3	GGTGAACATTCGAGGAAGCT	*5PTase13*-specific, amplification of total gene expression (Figure 7C)
	5PTase13 R3	AGGTTCGTGGGTCTGTTCTC	
At1g16610	SR45 F1	GCGATCACCTGATTCTCCC	*SR45*-specific, amplification of total gene expression (Supplemental Figure 4)
	SR45 R1	AGATCTATATCGTCTTGGAGG	
	SR45.1 F1	CGTCAGAAAGTATCTTCACCC	*SR45*-specific, amplification of *SR45.1* (Supplemental Figure 5A)
	SR45.1 R1	CTGTTTTCCGTTGAGGAGATG	
At1g29930	CAB1 F1	AGCCATCGTCACTGGTAAGG	*CAB1*-specific (Supplemental Figure 7)
	CAB1 R1	CCTCTCACACTCACGAAGCA	
At5G38410	RBCS3B F1	ACTCCCGGATACTACGATG	*RBCS3B*-specific (Supplemental Figure 7)
	RBCS3B R1	CTGATGCATTGGACTTGACG	
At3g18780	ACT2 F1	GGATCTGTACGGTAACATTGTGC	*Actin2*-specific, house-keeping gene (Figures 1A, 2A; Supplemental Figures 4, 5A)
	ACT2 R1	CTGCTGGAATGTGCTGAGG	
At5g60390	EF1A F1	TGAGCACGCTCTTCTTGCTTTCA	*EF1A*-specific, house-keeping gene (Figures 3B, 7C; Supplemental Figure 7)
	EF1A R1	GGTGGTGGCATCCATCTTGTTACA	

RT-PCR Analyses

Gene ID	Primer Name	Primer Sequence (5' to 3')	Description	# Cycles
At1g05630	5PTase13 F1	AGAAACGGTTGGACTTGAAGG	*5PTase13*-specific, amplification of *5PTase13.1* and *5PTase13.2* (Figure 7A, 7B)	33
	5PTase13 R1	ATAAGCTGAAGTTGAGACACC		
At3g01090	SnRK1.1 F1	TGCATTTTTTGGTTCCGAATTTTC	*SnRK1.1*-specific, amplification of *SnRK1.1.1*, *SnRK1.1.2* and *SnRK1.1.3* (Supplemental Figure 1)	30
	SnRK1.1 R1	CATCTCCATGTTCTTGATTTTG		
	SnRK1.1 F2	CAATGGATTGATCTTGAAATC	*SnRK1.1*-specific, amplification of *SnRK1.1.2* and *SnRK1.1.3* (Supplemental Figure 1)	30
	SnRK1.1 R2	ATAGAGACGGATGATGTGAGG		
	SnRK1.1 F3	GTCAAGTTTGAAATTCAGTTGT	*SnRK1.1*-specific, flanking T-DNA insertion in *snrk1.1-3* (Supplemental Figure 2B)	35
	SnRK1.1 R3	TTTAGTATTCAGAGGACTCGG		
At4g29130	HXK1 F2	GTTGGAGCGACTGTTGTTTG	*HXK1*-specific, flanking T-DNA insertions in *hxk1-1* and *hxk1-2* (Supplemental Figure 2A)	35
	HXK1 R2	ACTCTCGAAATCCAGCGTGT		
At1g16610	SR45 F1	AACGTTCACACTACCACCTCG	*SR45*-specific, flanking T-DNA insertion in *sr45-1* (Supplemental Figure 2)	35
	SR45 R1	GTAAGAAGATGACCTCCCACG		
At3g18780	ACT2 F2	TTTGCAGGAGATGATGCTCCC	*Actin2*-specific, house-keeping gene (Figure 7B; Supplemental Figures 1B, 2)	25
	ACT2 R2	GTCTTTGAGGTTTCCATCTCC		

Cloning

Gene ID	Primer Name	Primer Sequence (5' to 3')	Description
At1g16610	SR45 pBA F	TT*CTCGAG*ATGGCGAAACCAAGTCGTG	cloning of *SR45.1* to generate overexpressor lines (Supplemental Figure 4)
	SR45 pBA R	TT*AATTAA*AGTTTTACGAGGTGGAGGTGG	

Restriction sites are shown in italics and underlined.